ANALYSIS OF PERIODIC ORBITS ABOUT THE MARTIAN MOONS BY CONTINUATION TECHNIQUES

THESIS

Frank Luria, Captain, USAF

[redacted]

AFIT/GA/ENY/90D-10

ANALYSIS OF PERIODIC ORBITS ABOUT THE MARTIAN MOONS BY CONTINUATION TECHNIQUES

THESIS

Frank Luria, Captain, USAF

[redacted]

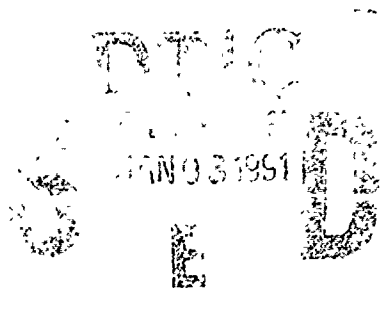

Approved for public release; distribution unlimited.

AFIT/GA/ENY/90D-10

ANALYSIS OF PERIODIC ORBITS ABOUT THE MARTIAN MOONS BY CONTINUATION TECHNIQUES

THESIS

Presented to the Faculty of the School of Engineering

of the Air Force Institute of Technology

Air University

In Partial Fulfillment of the

Requirements for the Degree of

Master of Science in Astronautical Engineering

Frank Luria, B.S.

Captain, USAF

December 1990

Acknowledgements

To my wife Renee whose love and support got me through this project and AFIT. I also thank my advisor Capt Jim Planeaux for much needed help.

Table of Contents

List of Figures

Appendix B

List of Tables

Notation

a,b,c	Axis Lengths of Moon
dM	Differential Element of Mass
d	Position Vector of the Satellite With Respect to Mars
D	Position Vector of the Moon With Respect to Mars
G	Universal Gravitational Constant
H	Hamiltonian
I_{xx}, I_{yy}, I_{zz}	Moon Mass Moments of Inertia
I_{xy}, I_{xz}, I_{yz}	Moon Mass Products of Inertia
L	Lagrangian
M,m	Mass
P_i	Generalized Momenta
Q_i	Generalized Coordinates
r	Position Vector of the Satellite With Respect to dM
R	Position Vector of the Satellite With Respect to the Moon
T	Kinetic Energy
v	Velocity
V	Potential Energy
x	Moon's Minimum Axis of Inertia
y	Moon's Intermediate Axis of Inertia
z	Moon's Maximum Axis of Inertia
Ω	Rotation Rate of Moon
μ	Density of Moon

Abstract

From a few known periodic orbits of Phobos and Deimos and Deimos, continuation techniques were used to find entire families ofstable orbits. These techniques involved varying a parameter,the Hamiltonian, of the system and analyzing how the orbital behavior changed with the parameter. Floquet multipliers, for stability analysis, were also computed. AUTO86, a continuation and bifurcation software package, was used in this study. Artificial energy dissipation had to be added to the conservative Hamiltonian system to enable use of AUTO.

I. Introduction

Several stable orbits about two natural satellites of Mars, Phobos and Deimos, were found by Jansson (4:28) using Poincare's surface of section technique. This study was accomplished to compute additional stable orbits about both moons by using analytic continuation methods. It was hoped that, using continuation methods with bifurcation analysis, families of stable periodic orbits could be found.

The same modified restricted three body model and equations of motion were used to describe the Mars, moon, and artificial satellite system. A solution, in this case a previously found stable periodic orbit, was used to start the continuation process. A software package, AUTO86, was then used to compute stable and unstable orbits of various periods using continuation methods. Stability was determined by analyzing the Floquet multipliers, which were computed for each test case.

Along with finding stable orbits, bifurcation analysis was accomplished on the solution branches to characterize the behavior of the nonlinear equations of motion. Using this approach, bifurcating orbits of higher period were sought; unfortunately none were found.

The various stable orbits found about Phobos and Deimos will be presented. Also, stable orbit behavior versus changing system parameters will be demonstrated.

II. Continuation Methods

Theory

The basis for being able to find solutions to the non-linear equations of motion is the numerical technique of continuation. Continuation is the process of starting from a known solution and varying a parameter contained in the system. As this parameter is varied in small increments, previous solutions starting from the known solution are used to approximate new solutions. Since the increments are small, the iteration to compute the new solutions should converge rapidly.

To illustrate the idea of continuation, take an algebraic system

$$\phi(x)=0 \tag{1}$$

with a known solution B, and introduce into it a parameter λ. A new system is formed (1:18)

$$G(\lambda,x)=\lambda f(x)+(1-\lambda)\phi(x)=0 \tag{2}$$

For λ=0, the known solution x=B is reverted to. For λ=1, the system becomes

$$f(x)=0 \tag{3}$$

which is the system we want to solve. The "continuation path" in λ is

$$0=\lambda_1<\lambda_2<\lambda_3\ldots<\lambda_q=1 \tag{4}$$

where λ is incremented in small steps. $X(\lambda_1)=B$ is known and is used to approximate $x(\lambda_2)$, similarly $x(\lambda_i)$ approximates $x(\lambda_{i+1})$, for i=1,2,..q-1. Since the parameters λ_i are close to one another, the iteration used to solve for $x(\lambda_{i+1})$ should converge rapidly.

Nonlinear Analysis

Continuation of a starting solution can tell you many things about how a nonlinear system of equations behaves. For instance, suppose from the known solution, additional solutions vary continuously (call this a solution branch) to a certain value of λ. After this value of λ, the solution branch "splits off" into multiple branches. This splitting off is known as bifurcation. The point at which the number of solutions changes as a certain value of the parameter is passed is called a branch point (8:40). It can be seen how the nonlinear system behaves as the parameter is varied if the solution is plotted versus the parameter. This is known as a bifurcation diagram. Bifurcation theory involves analyzing and interpreting the solution branches of a bifurcation diagram.

In the above example, the solution branch mapped out solutions to the algebraic system of Equation (1). An equilibrium solution branch resulted, with each point on the branch being an equilibrium point. This study is concerned with continuation of the first order ordinary differential set

of equations that describe the motion of an artificial satellite about a Martian moon. These equations are of the form

$$\dot{X}=f(X,\lambda) \tag{5}$$

where λ is again the continuation parameter introduced into the system. For this system, any point where

$$\dot{X}=0 \tag{6}$$

is called an equilibrium point. Therefore, the solution branches for this system do not necessarily map out equilibrium points. Periodic solution branches, which will be discussed in the next section, could also be computed. However, it is still true that bifurcations result when the solution branch divides into multiple paths.

Besides dividing into multiple paths, the solution branch may, at a certain value of the parameter, actually turn back and follow a different path. The point where it turns back is another branch point known as a limit point. Figure 1 shows the branch points discussed and how the solutions to a nonlinear set of equations can behave. Of particular interest to this study is the investigation of periodic solutions to a set of ordinary differential equations.

Periodic Solutions

A periodic solution to a set of equations in the form of Equation (5) is described by

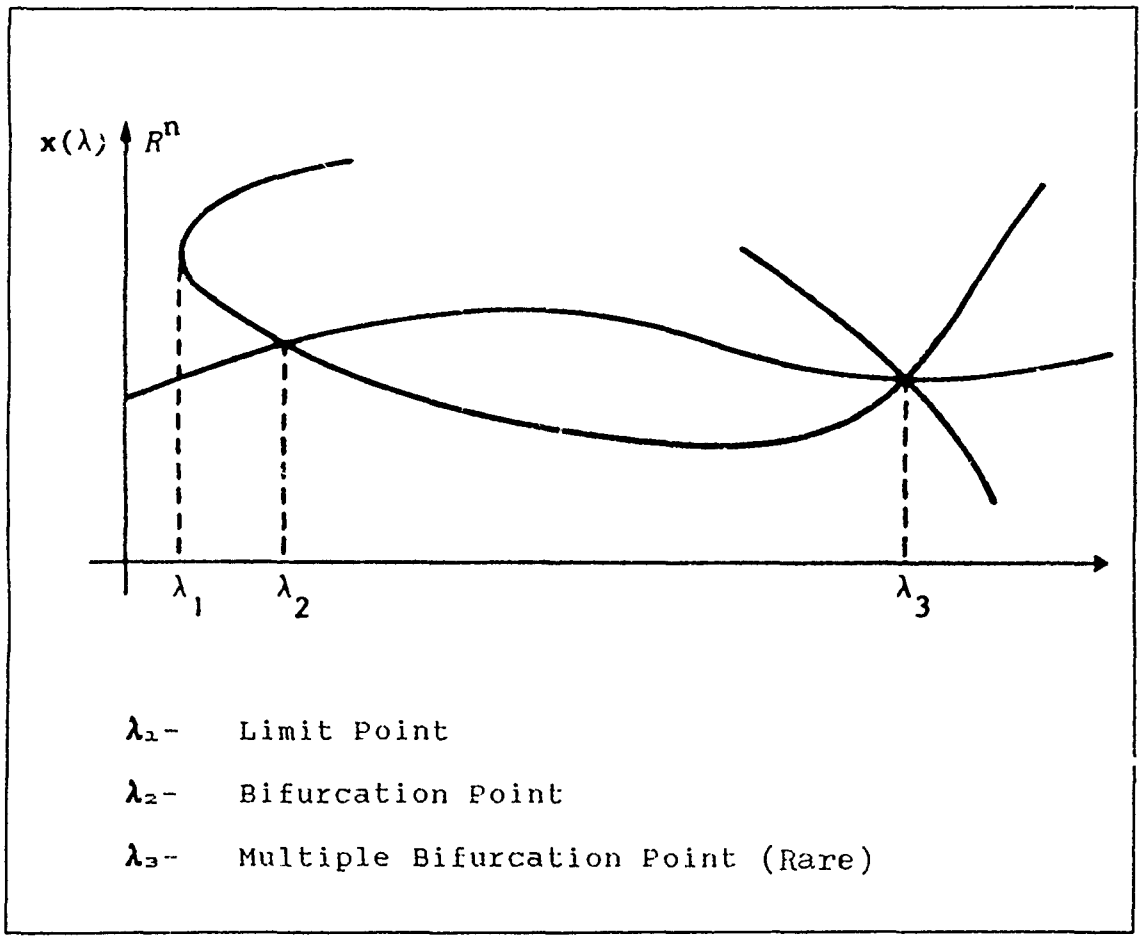

Figure 1. Branch Points on Bifurcation Diagram (1:44)

$$X(t+T)=X(t) \tag{7}$$

where T is the period and t is the time. Equation (5) represents an autonomous system because the time variable does not appear in $f(x,\lambda)$ (5:81). An isolated periodic solution is known as a limit cycle and is represented by a closed curve in the phase plane for a two dimensional system, the phase plane being the solution plane with the system state variables as its axes. An example of this would be a diagram of a periodic orbit about Phobos. This orbit would represent a periodic solution to the nonlinear equations of the system and would appear as a closed curve when plotted in its orbital plane. After each period, T, the orbit would return to its original starting position. The idea of orbital stability will now be addressed.

Stability

A periodic solution is stable if, with increasing time, all trajectories in its neighborhood end up on the trajectory (6:26). With periodic solutions, stability is determined by computing Floquet multipliers.

Floquet multipliers are simply eigenvalues of a special matrix called the monodromy matrix. The monodromy matrix of the periodic solution $X^*(t)$ with period T and initial vector Z^* is defined by

$$M=\Phi(T)=\frac{\partial \Phi}{\partial Z}(T;Z^*) \tag{8}$$

where (8:240-241)

$$\Phi(t;Z) \tag{9}$$

is the solution to

$$\dot{X}=f(X,t),X(0)=Z \tag{10}$$

and

$$\dot{\Phi}=f_x(x^*,t)\Phi,\Phi(0)=I \tag{11}$$

If the magnitude of any of the Floquet multipliers is greater than one, then the periodic orbit is unstable. In general, the Floquet multipliers, hence the stability vary with the parameter λ (8:248).

In a conservative Hamiltonian system, periodic solutions appear as closed paths in the phase plane (two dimensional system) and do not approach a limit cycle. Each multiplier in this system will have a magnitude of one.

Method Using AUTO86

The continuation methods used in this study were accomplished with the continuation/bifurcation software package AUTO86, written by Eusebius Doedel. AUTO was used to compute stable or unstable periodic solutions to the nonlinear ordinary differential equations of this study. To do this, the package takes a known periodic solution and uses continuation to compute solution branches. The Floquet multipliers, which indicate stability as discussed earlier, are also computed. As the solution branches are continued,

AUTO searches for limit points, bifurcation points, and other branch points. It also has the capability to restart the continuation along a desired solution branch at a bifurcation point.

AUTO requires user supplied subroutines, which include the system equations of motion, a steady state or periodic solution at a certain parameter value, and user determined program constants. Pseudo arclength continuation is then performed to compute solution branches. Arclength continuation is used to compute past limit points on a branch where other methods sometimes fail. As an example of pseudo arclength continuation (2:12-14), the solution (u_{j-1},p_{j-1}), where p is a parameter of

$$f(u,p)=0 \tag{12}$$

is known along with its direction (du_{j-1},dp_{j-1}). From the set of equations

$$f(u_j,p_j)=0 \tag{13}$$

$$\theta^2{}_u(u_j-u_{j-1})\dot{u}_{j-1}+\theta^2{}_p(p_j-p_{j-1})\dot{p}_{j-1}-ds=0 \tag{14}$$

where ds is the stepsize along the branch, the next solution (u_j,p_j) is computed. The stepsize ds can either be fixed or adaptive. If it is adaptive and the Newton iteration scheme converges rapidly, ds is increased for the next solution. If the iteration fails to converge, the stepsize, if adaptive, is halved. This continues until convergence is reached or the

stepsize reaches a predetermined minimum value. This practice is also used for the continuation of periodic solutions.

AUTO computes the Floquet multipliers by applying a standard eigenvalue routine. The number of Floquet multipliers inside the unit circle is monitored. For the periodic case, there is always a multiplier on the unit circle, specifically at +1 (2:48). If any multipliers are outside the unit circle, the solution is unstable. If all the multipliers are on the unit circle, as in a conservative Hamiltonian system, the solution is neutrally stable.

III. System Dynamics

Description

The system in this problem consists of a natural satellite, Phobos or Deimos, in a circular orbit about Mars. The artificial satellite is then orbiting Phobos or Deimos. It is assumed that the mass of the artificial satellite is small and does not affect the motion of Mars or the moons. This situation is known as the restricted three body problem. The coordinate system, seen in Figure 2, consists of the moon centered orthogonal axes x,y, and z. The angular velocity of each moon about Mars is such that in one period, the moon will have also rotated about its spin axis once. Therefore, the x-axis is always pointing away from Mars. The y-axis is tangent to the moon's orbit about Mars, the orbit being in the x-y plane. The moons rotate about the z-axis, which completes the orthogonal set of axes.

Mars and the artificial satellite are considered symmetric spheres (x,y, and z moments of inertia are equivalent). However, the moons Phobos and Deimos are modeled as triaxial ellipsoids. Each moon rotates about its maximum axis of inertia (z-axis). Because of the asymmetric non-spherical moons, this becomes a modified restricted three body problem. The values of the constants used to derive the equations of motion and other system parameters for Mars, Phobos, and Deimos are contained in Appendix A.

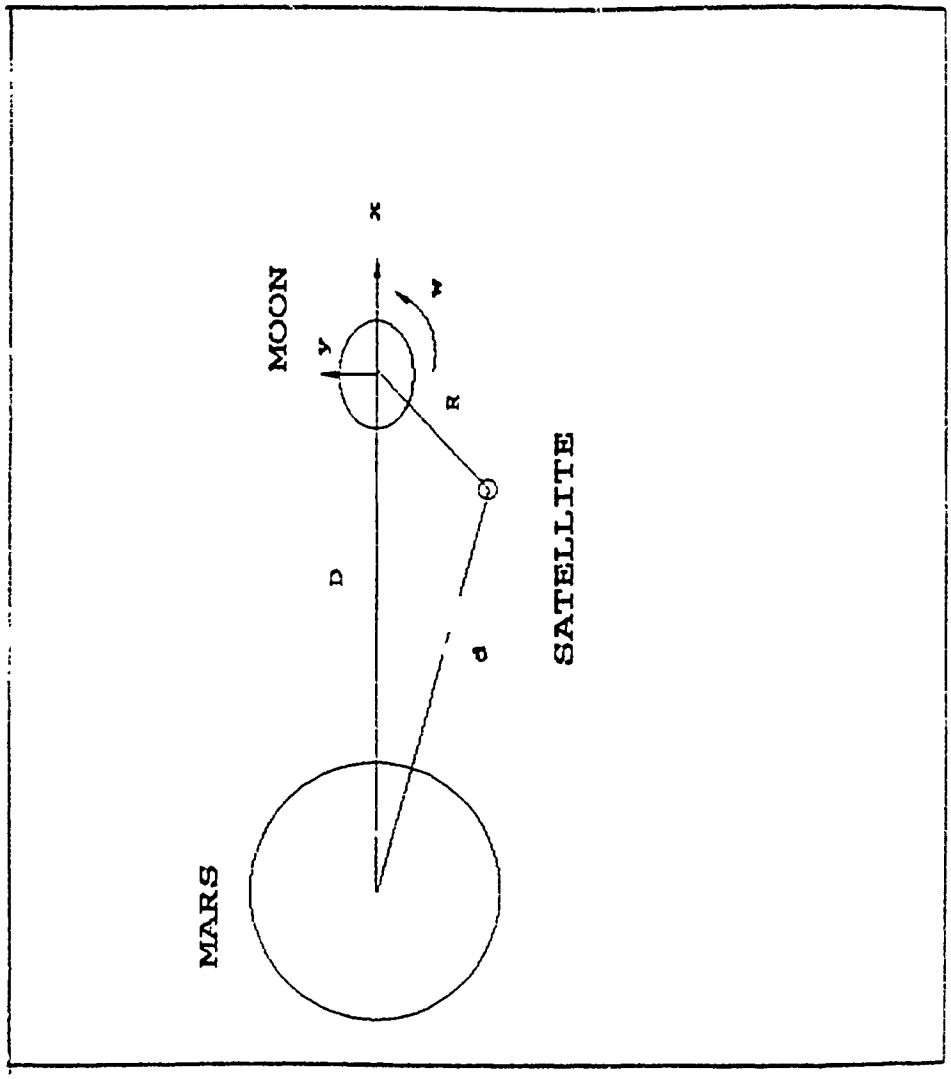

Figure 2. Coordinate System

Equations of Motion

The equations of motion for this system are shown below.

$$\dot{X}=P_x+\Omega Y \tag{15}$$

$$\dot{Y}=P_y-\Omega(X+D) \tag{16}$$

$$\dot{Z}=P_z \tag{17}$$

$$\begin{aligned}\dot{P}_Y=&-\Omega P_x-GM_{mars}d^{-3}Y-GM_{moon}R^{-3}Y\\&+\frac{3}{4}GR^{-5}Y(3I_{xx}+3I_{zz}-I_{yy})\\&-\frac{15}{4}GR^{-7}Y[X^2(I_{yy}+I_{zz}-I_{xx})\\&+Y^2(I_{xx}+I_{zz}-I_{yy})+Z^2(I_{xx}+I_{yy}-I_{zz})]\end{aligned} \tag{18}$$

$$\begin{aligned}\dot{P}_x=&\Omega P_y-GM_{mars}d^{-3}(X+D)-GM_{moon}R^{-3}X\\&+\frac{3}{4}GR^{-5}X(3I_{yy}+I_{zz}-I_{xx})\\&-\frac{15}{4}GR^{-7}X[X^2(I_{yy}+I_{zz}-I_{xx})\\&+Y^2(I_{xx}+I_{zz}-I_{yy})+Z^2(I_{xx}+I_{yy}-I_{zz})]\end{aligned} \tag{19}$$

$$\begin{aligned}\dot{P}_z=&-GM_{mars}d^{-3}Z-GM_{moon}R^{-3}Z\\&+\frac{3}{4}GR^{-5}Z(3I_{xx}+3I_{yy}-I_{zz})\\&-\frac{15}{4}GR^{-7}Z[X^2(I_{yy}+I_{zz}-I_{xx})\\&+Y^2(I_{xx}+I_{zz}-I_{yy})+Z^2(I_{xx}+I_{yy}-I_{zz})]\end{aligned} \tag{20}$$

These equations of motion were derived from Hamilton canonical equations and are identical to the equations used in previous studies. This study restricts the satellite to two degrees of freedom, or motion in the x-y plane. Therefore,

for this analysis, z=0, and the equations concerning z are to be ignored.

Since the Lagrangian found does not contain time, t, explicitly, the Hamiltonian, H, is constant and defined as

$$H=\sum_{k=1}^{n} \frac{\partial L}{\partial \dot{q}_k}\dot{q}_k-L=const \tag{21}$$

where H also constitutes an integral of motion known as Jacobi's integral (4:19). Because this system is nonnatural, Jacobi's integral replaces the energy integral as a constant of the motion. This system is nonnatural because the satellite's kinetic energy is

$$T=1/2m[(\dot{X}-\Omega Y)^2+(\dot{Y}+\Omega X+\Omega D)+\dot{Z}^2] \tag{22}$$

which is not a homogeneous quadratic function of the generalized velocities. The resulting Hamiltonian is of the form

$$H=1/2m(P_x^2+P_y^2)+\Omega(YP_x-XP_y)+V \tag{23}$$

which is characteristic of the restricted three body problem (7:422). In this modified problem the generalized velocities are

$$\dot{X}=P_x+\Omega Y \tag{24}$$

$$\dot{Y}=P_y-\Omega(X+D) \tag{25}$$

The fact that Jacobi's integral is a constant of motion enabled stable orbits about the moons to be found (4:1).

Known Periodic Solutions

For different values of the Hamiltonian, stable periodic orbits were previously found for both Phobos and Deimos (4:28). Table I lists the orbits that were simple and closed in nature. More periodic orbits were actually discovered, but the majority rotated and precessed about the moons and took several revolutions to complete one orbit. From Figure 3, it is seen that the starting point of all stable orbits found was on the negative x-axis, and the orbital motion was retrograde with respect to the rotation rate of the moons.

Table I. Simple, Closed Orbits Previously Found (4:33,50)

PHOBOS			DEIMOS		
H	S.P.	PERIOD	H	S.P.	PERIOD
-6.8528	-22,0	13,900	-2.738592	-10,0	18,800
-6.8527	-68,0	26,600	-2.738591	-13,0	25,800
-6.8526	-93,0	27,200	-2.738590	-18,0	35,400
-6.8525	-112,0	27,400	-2.738589	-23,0	53,600
-6.8524	-129,0	27,400	-2.738588	-31,0	72,100
-6.8523	-143,0	27,500	-2.738587	-41,0	83,200
-6.8522	-156,0	27,500	-2.738586	-48,0	90,800
-6.8521	-169,0	27,400	-2.738585	-56,0	93,000
-6.8520	-179,0	27,600	-2.738580	-75,0	106,000
-6.8500	-332,0	27,600	-2.738570	-109,0	108,000
-6.8400	-708,0	27,500	-2.738560	-135,0	108,000
			-2.738550	-156,0	108,000
			-2.738500	-233,0	109,000
			-2.738400	-340,0	109,000
			-2.738300	-418,0	109,000

H- Hamiltonian Value, km^2/sec^2
S.P.- (x,y) Starting Point of Orbit, km
Period- Period of Orbit, sec

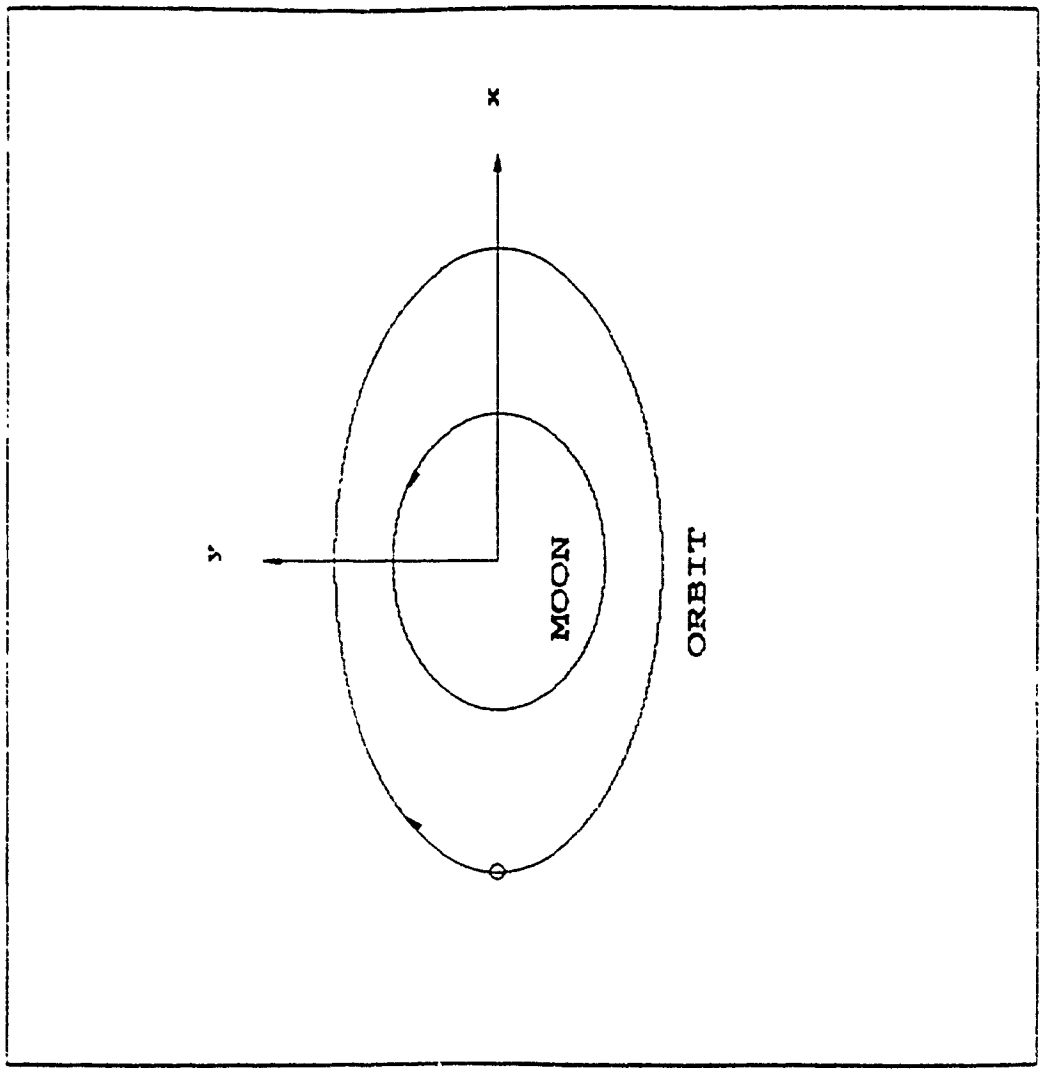

Figure 3. Typical Stable Orbits Found

IV. Solution Approach

Starting Solutions

As mentioned in section II, the numerical continuation package AUTO requires the system equations of motion and a starting periodic solution. Figure 4 shows the periodic solutions used to start AUTO for both Phobos and Deimos. These were the closest stable, closed orbits previously found about the moons. As mentioned earlier, these orbits are retrograde (clockwise) with respect to the rotation of the moons. The period of the orbit about Phobos is approximately 14,000 seconds, which is about half of the Phobos period about Mars. The period of the orbit about Deimos is approximately 19,000 seconds. The period of Deimos about Mars is about 108,000 seconds.

Equation Modification

The equations for this Hamiltonian system are conservative. It seems from previous work that there is a continuum of solutions, simple closed orbits, as the Hamiltonian changes value. In a system with naturally occurring free parameters, AUTO is designed to compute periodic solutions that arise from bifurcation from a stationary solution, a Hopf bifurcation (2:1). AUTO works best with nonconservative systems which have some type of energy dissipation. This Hamiltonian system conserves energy. This system was thus modified to make efficient use of AUTO.

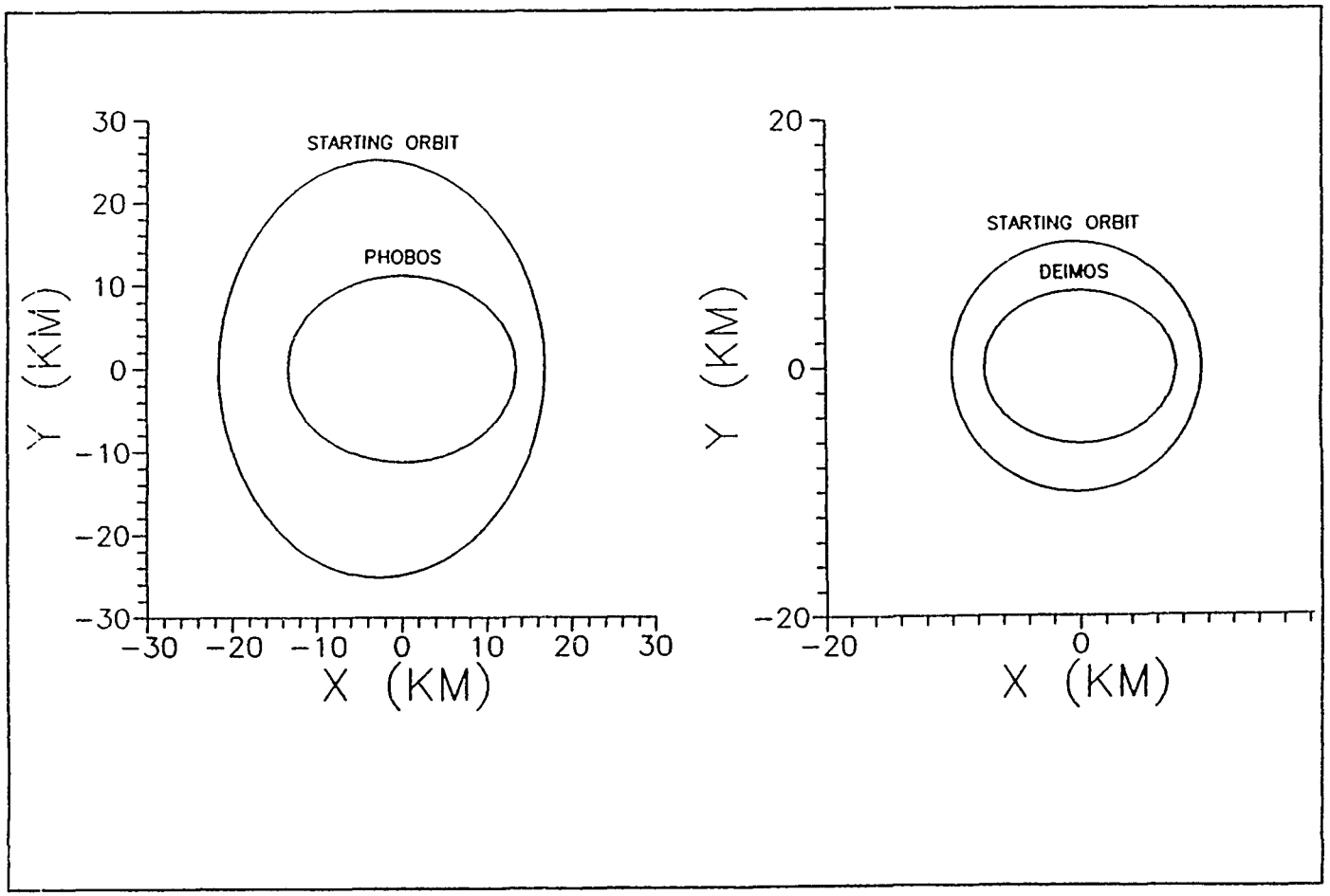

Figure 4. Starting Periodic Solutions

Since there is no naturally occurring free parameter in the equations of motion, one was needed. The second equation of motion, Equation (16), could be rewritten in terms of the Hamiltonian H,

$$\dot{y}=\frac{P_y^2-P_x(2\Omega Y+P_x)+2H-2V}{2P_y} \tag{26}$$

However, making H the parameter here results in too much of a change to the system when AUTO varies it; no solutions are computed. The system was then modified to add artificial energy dissipation. This dissipation term

$$\frac{\partial H}{\partial P_y}(H_o-H(X,Y,P_x,P_y)) \tag{27}$$

was added to the fourth equation of motion

$$\dot{P}_y=-\frac{\partial H}{\partial Y}+\frac{\partial H}{\partial P_y}(H_o-H(X,Y,P_x,P_y)) \tag{28}$$

AUTO varies H_0 as the continuation parameter and the Hamiltonian value, $H(X,Y,P_x,P_y)$, is constant on a specific orbit. Part of the dissipation term

$$\frac{\partial H}{\partial P_y} \tag{29}$$

is actually the second equation of motion, the velocity in the y-direction. The initial value of H_0 is the Hamiltonian value for the starting solution. At this solution, $H_0 = H(X,Y,P_x,P_y)$, therefore the dissipation term equals zero. As AUTO varies H_0, a small amount of dissipation is added to the system and

AUTO looks for solutions to the changed system. The added dissipation forces the solutions to be in the three dimensional subspace of $H_0=H(X,Y,P_x,P_y)$, but the solutions still behave as conservative once in this subspace. With this term added, AUTO had no trouble locating stable periodic orbits for a wide range of parameter values. This artificial energy dissipation term was not the only term that could be used, but it did provide satisfactory results.

Output Interpretation

Output from AUTO consisted of initial x and y values of orbits found, associated parameter values (Hamiltonian in this case), maximum x and y values along the trajectory, the orbital period, and stability information including Floquet multipliers and the number of multipliers inside the unit circle. Plots of the trajectories were made by numerically integrating the initial x,y,P_x, and P_y values of the orbits computed, along with the Hamiltonian value and period. The Haming Integrator, which contains a fourth order predictor corrector algorithm (9:108), was used to numerically integrate the trajectories. Many continuation runs were accomplished for both Phobos and Deimos to seek periodic orbits and nonlinear behavior patterns. The solutions found for both Phobos and Deimos will be discussed in the next section.

V. Results and Discussion

Phobos

Running AUTO with the equations of motion plus the artificial energy dissipation term resulted in a wide range of stable orbits found. As the continuation parameter, the system Hamiltonian H, was varied, a continuum of stable orbits were computed. The first objective of this study was to verify the stable periodic orbits found in previous work.

Stable Orbit Verification. Table II lists a sampling of the stable orbits found using AUTO continuation methods. Many more were found between the H values listed in the table. As the parameter H increased, the starting point for the orbit moved away from the origin of the moon. This means that the major axis of each orbit, which lies on the x-axis as seen in Figure 2, increased for increasing Hamiltonian values. Also, the orbital periods increased as the parameter H increased until a certain period was reached. This period was 27,557 seconds, which is approximately the orbital period of Phobos about Mars. These results agreed with previous work using Poincare's surface of section technique. Figure 5 shows the orbits found which were closest to the surface of Phobos. The parameter value for the closest orbit found was H=-6.852806. Many more orbits were computed with a lower parameter value, but these orbits "collided" with Phobos when integrated around their trajectories.

Table II. Stable Orbits Computed About Phobos
Ω =.000228 r/s

H	INITIAL X	R_p	R_a	e	PERIOD
-6.852806	-17.9	13.7	19.0	.16	11,000
-6.85280	-21.5	16.8	25.2	.20	13,901
-6.85275	-50.1	43.8	87.9	.33	25,424
-6.85270	-67.4	60.9	125.0	.34	26,676
-6.85265	-80.8	74.2	152.6	.35	27,050
-6.8526	-93.1	86.4	177.7	.35	27,229
-6.85257	-99.2	92.4	190.3	.35	27,288
-6.8517	-212.7	205.8	418.5	.34	27,532
-6.8502	-318.7	312.0	630.3	.34	27,550
-6.84761	-450.2	442.6	892.9	.34	27,555
-6.84425	-576.5	568.8	1145.3	.34	27,557
-6.8400	-706.5	700.0	1399.6	.33	27,557
-6.8300	-939.2	932.4	1872.8	.34	27,558
-6.8259	-1018.7	1008.8	2029.5	.34	27,557
-6.8203	-1119.0	1112.3	2229.5	.33	27,558
-6.8104	-1277.3	1270.5	2537.3	.33	27,558
-6.8000	-1431.9	1424.9	2807.1	.33	27,558
-6.7850	-1615.6	1601.0	3203.9	.33	27,558
-6.768	-1804.6	1789.3	3570.2	.33	27,557
-6.748	-2006.0	1986.9	4103.3	.35	27,555

H- Hamiltonian, km^2/s^2
R_p, R_a- Pericenter, Apocenter Distances, km
e- eccentricity
PERIOD- Period, seconds

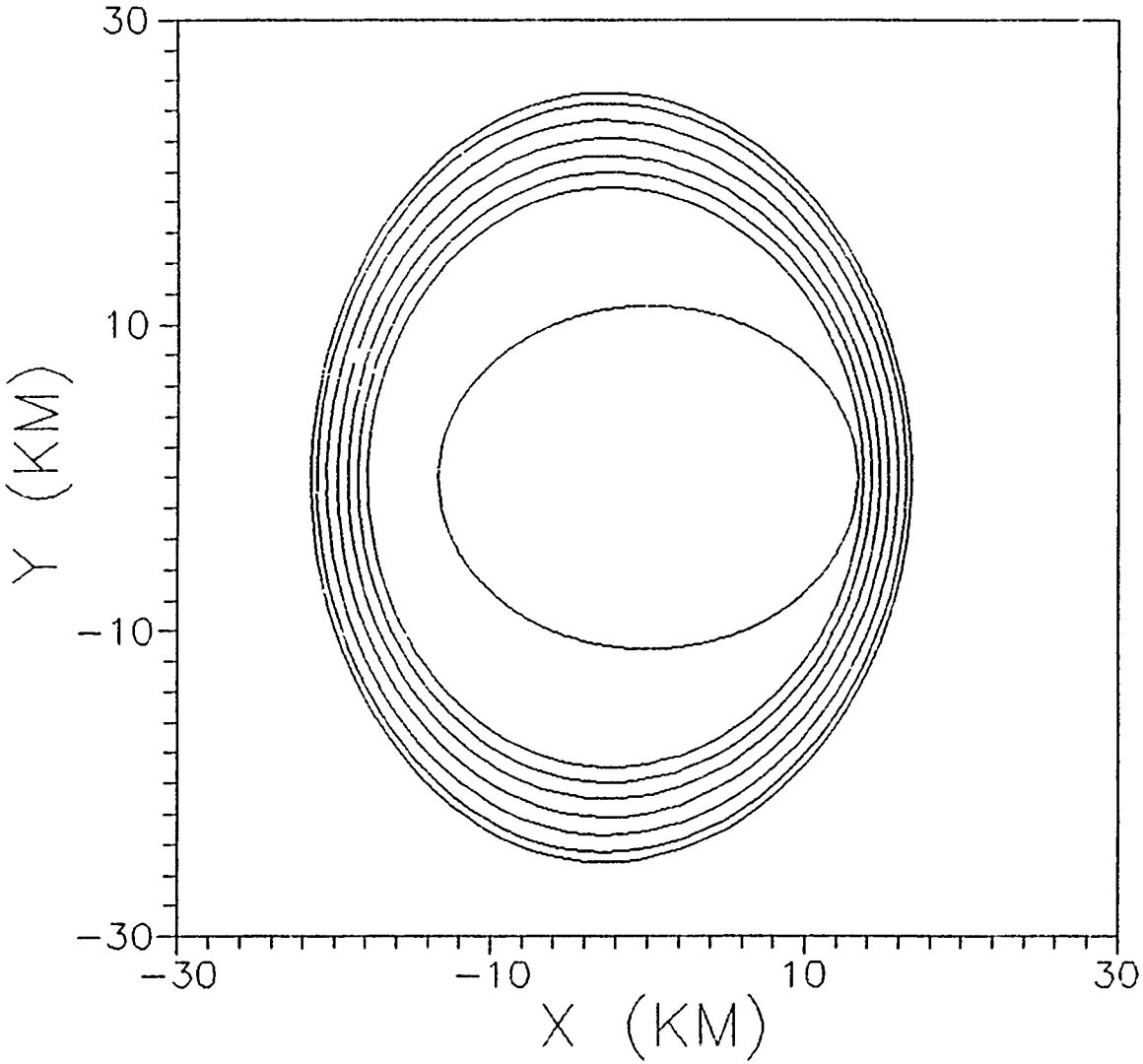

Figure 5. Orbits Closest to Phobos, Ω=.000228 r/s

Figure 6 shows the orbits computed that were furthest from Phobos. All of these orbits have the same orbital period as Phobos. Since the periods are identical, the largest orbit shown must have much higher orbital velocities than the smallest. The largest orbit, with a major axis of 6090.2 km has an initial velocity in the y-direction of 975 m/sec compared to the smallest orbit, major axis of 2014.8 km, with initial velocity 313 m/sec. These larger orbits are basically in orbit about Mars, being much less perturbed than the closer orbits.

Figure 7 shows how the initial x,y position of the stable orbits computed varied as the parameter H was varied. The squares represent the orbits found by continuation and the triangles represent the orbits previously found. It is seen that the two curves formed lie on top of each other. This shows that the continuation methods used in this study did indeed agree with other methods used. In addition, more stable orbits were found at regular intervals of the Hamiltonian values.

Resonant Orbits. An attempt was made to characterize resonant orbits found in a previous study. A previously found resonant orbit, shown in Figure 8, encircled Phobos seven times before returning to its starting point. This orbit was used to search for other resonant orbits. The results, shown in Table III, were only marginally successful. Several larger

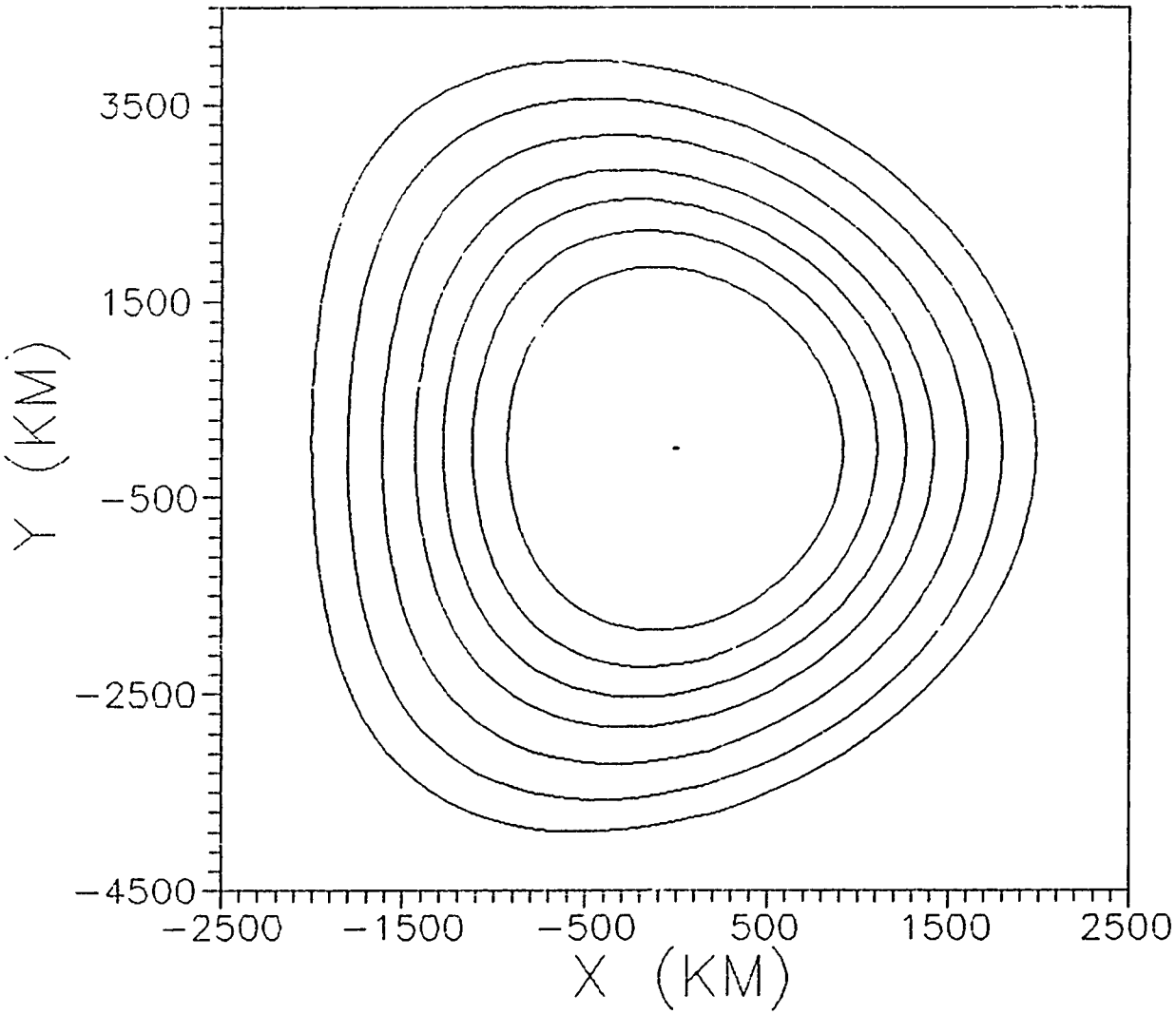

Figure 6. Orbits Furthest from Phobos, Ω=.000228 r/s

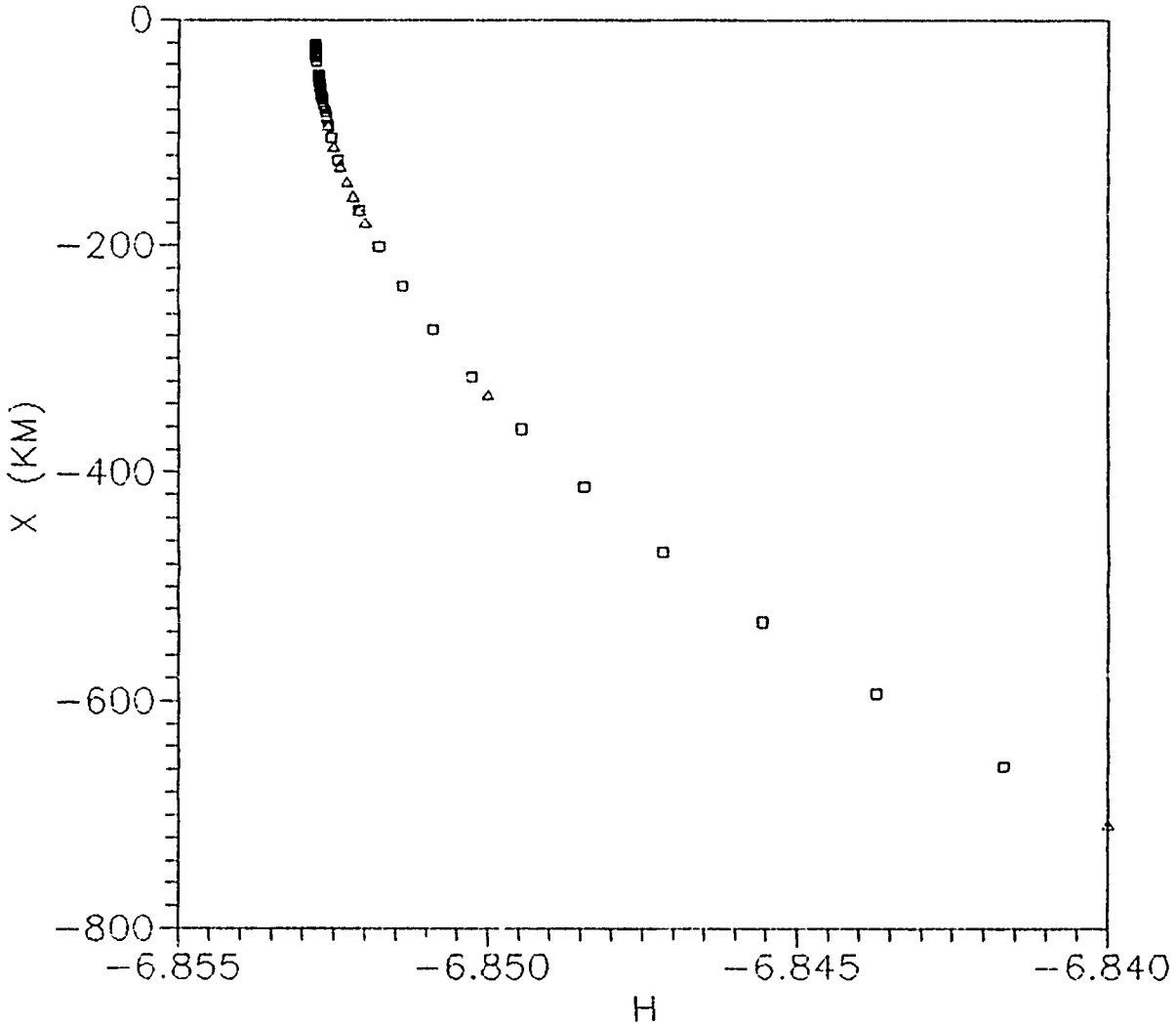

Figure 7. Comparison of Computed vs Previous Orbits for Phobos

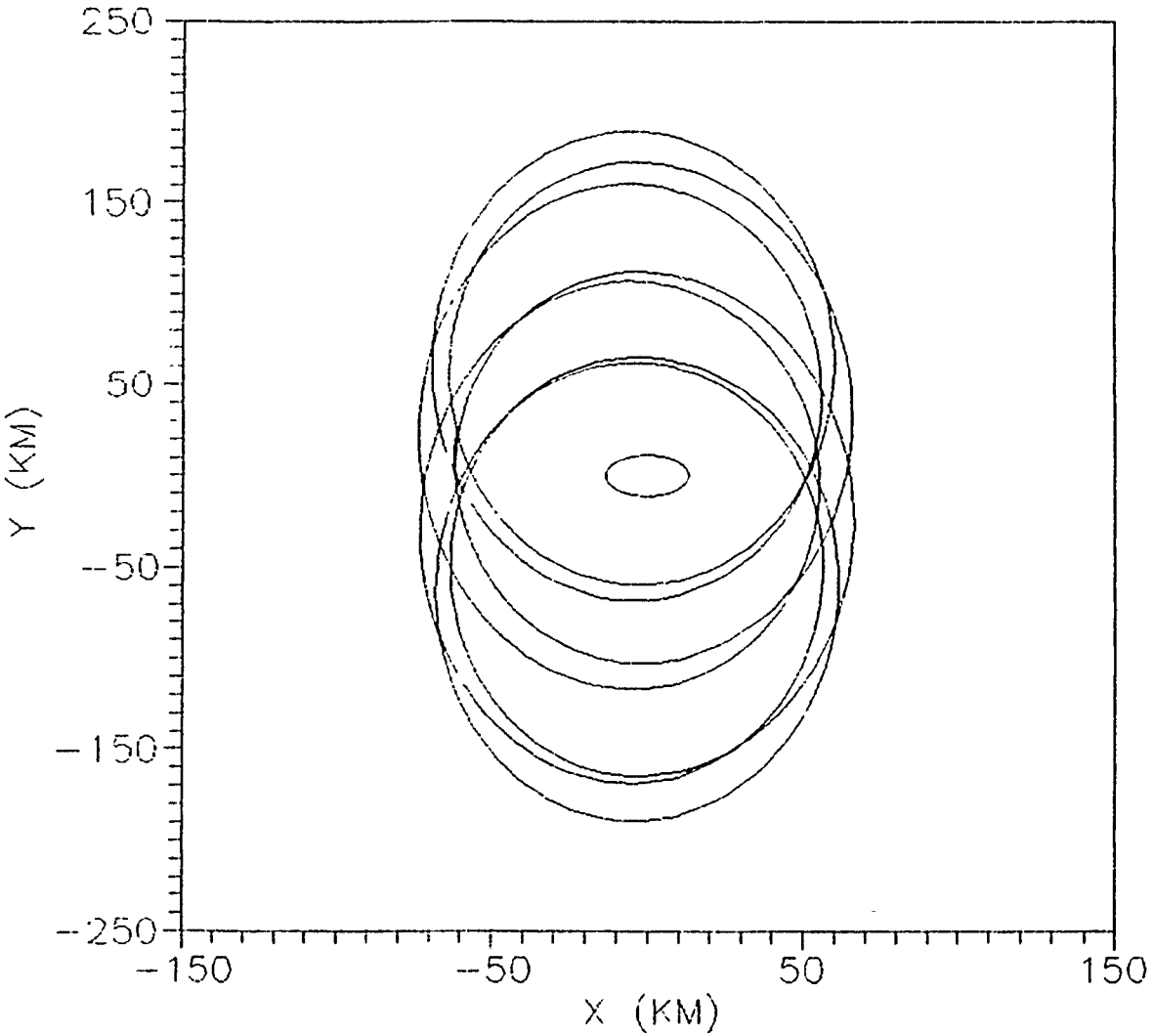

Figure 8. Phobos Resonant Orbit, H= -6.8527

Table III. Resonant Orbits of Phobos

H	INITIAL X	MAX X	MIN X	MAX Y	PERIOD
-6.85270	-62.0	66.3	-73.2	189	186,200
-6.85269	-64.0	72.2	-78.8	217.2	186,200
-6.85264	-64.6	73.3	-80.0	222.2	186,309
-6.85268	-65.4	74.7	-81.4	228.6	186,449
-6.852674	-66.6	76.9	-83.6	237.6	186,641

H- Hamiltonian Value, km^2/s^2
X- X value, km
Y- Y value, km
PERIOD- Period, seconds

orbits of the same variety, seven encirclements, were found. Again, following the same pattern of the single encirclement stable orbits, as the parameter H increased, the size of the orbits increased. After these few orbits were computed, further solutions found were of the single revolution type. It was hoped that a bifurcation would be seen here. Perhaps AUTO failed to detect the phenomena which led back to the continuation of single revolution orbits. Therefore, no definite pattern was found to these resonant orbits. Nothing can be said of any higher order resonant orbits, although their existance was indicated through a previous study (4:43).

Rotation Rate Effects. If this is considered a two body problem with the satellite orbiting Mars, the value for the rotation rate of Phobos is calculated to be Ω_{new}=.00022788 rad/s. This was calculated by setting x=y=0, omitting the moon terms, then solving for the rotation rate, Ω . However, the stable orbits found thus far assumed Ω_{old}=.000228 rad/s, evidently a rounded off approximation. Continuation methods were used to find stable orbits for Ω_{new}. Figure 9 illustrates the results of decreasing Phobos' rotation rate to its true value. The smallest orbit, whose perigee point is on the x-axis closest to the surface of Phobos, was computed from Ω_{old}. As this rotation rate is decreased to Ω_{new}=.00022788 rad/s, the perigee point moves away from Phobos for the same starting point, which is

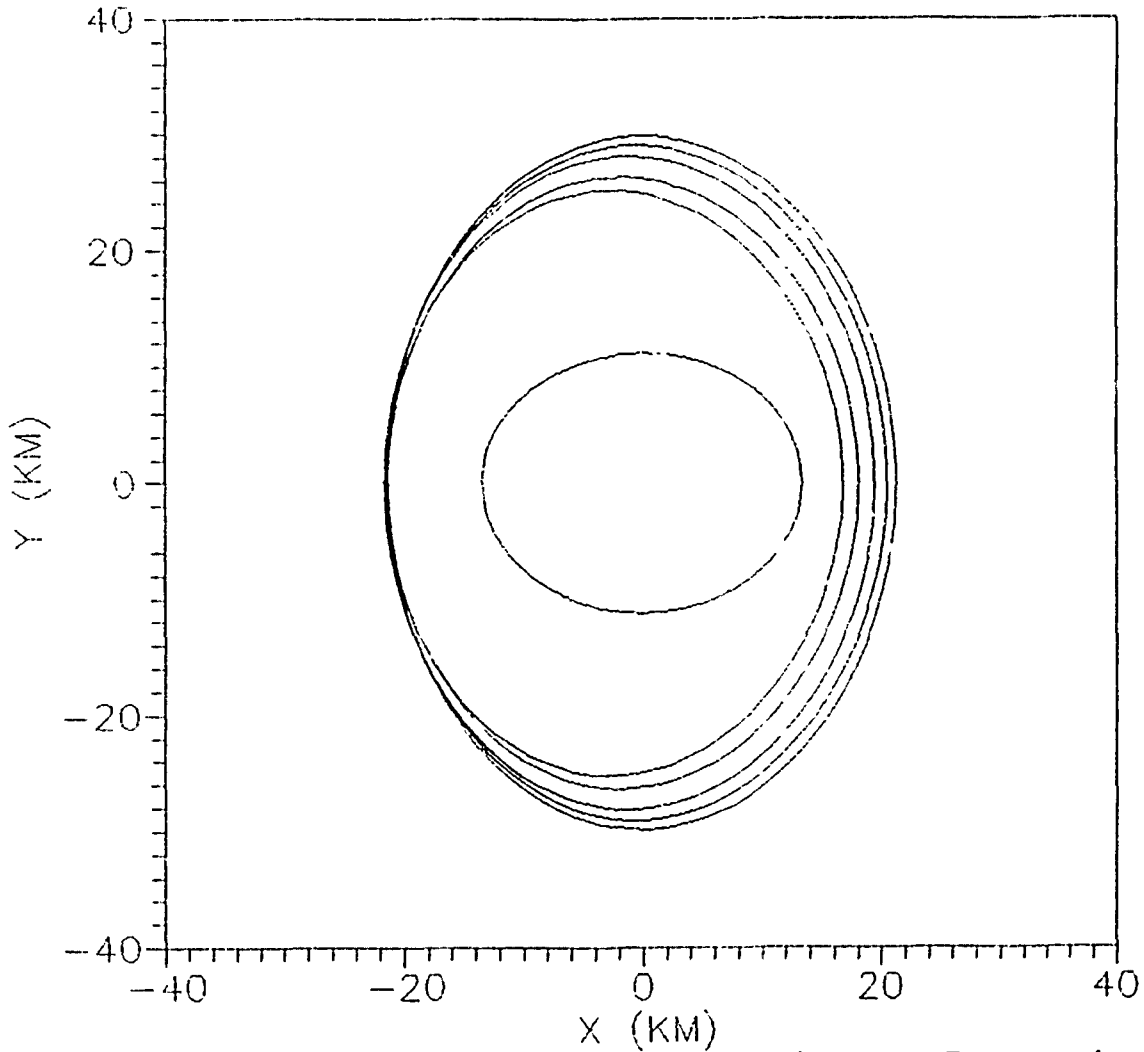

Figure 9. Phobos Orbits Corresponding to Decreasing Rotation Rate

approximately (x,y)=(-22km,0km). This also results in the orbits becoming centered on Phobos. The rotation rate of Phobos is assumed to be .00022788 rad/s for all further analysis. Figure 10 again shows the effects of this change in rotation rate. For the higher rotation rate, the x value for the starting point of the stable orbit is larger than for the smaller rotation rate. This means that as the Phobos rotation rate is less accurately modeled, at a certain value of H, the stable orbit becomes larger. For example, at H=-6.8481, the major axis of the stable orbit computed is 1267 km for the faster rotation, compared to 893 km for the slower rotation. It seems that as the largest values of H are approached, these differences diminish. This is shown by Figure 11. Both curves start separately at the initial H value of -6.855, but seem to converge as H increases to -6.755. The major axis, in both cases, approaches 5400 km. Qualitatively, the effects of correcting the value of Ω are small, but the smallest orbits are affected rather significantly.

Table IV summarizes the range of stable orbits centered on Phobos that were computed. Again, the periods converged to Phobos' period. Figure 12 shows the orbits found that were closest to Phobos. Figure 13 displays the orbits that were furthest from the moon. As in the case with the higher rotation rate, all of these larger orbits are essentially in a Martian orbit and are only slightly perturbed by Phobos.

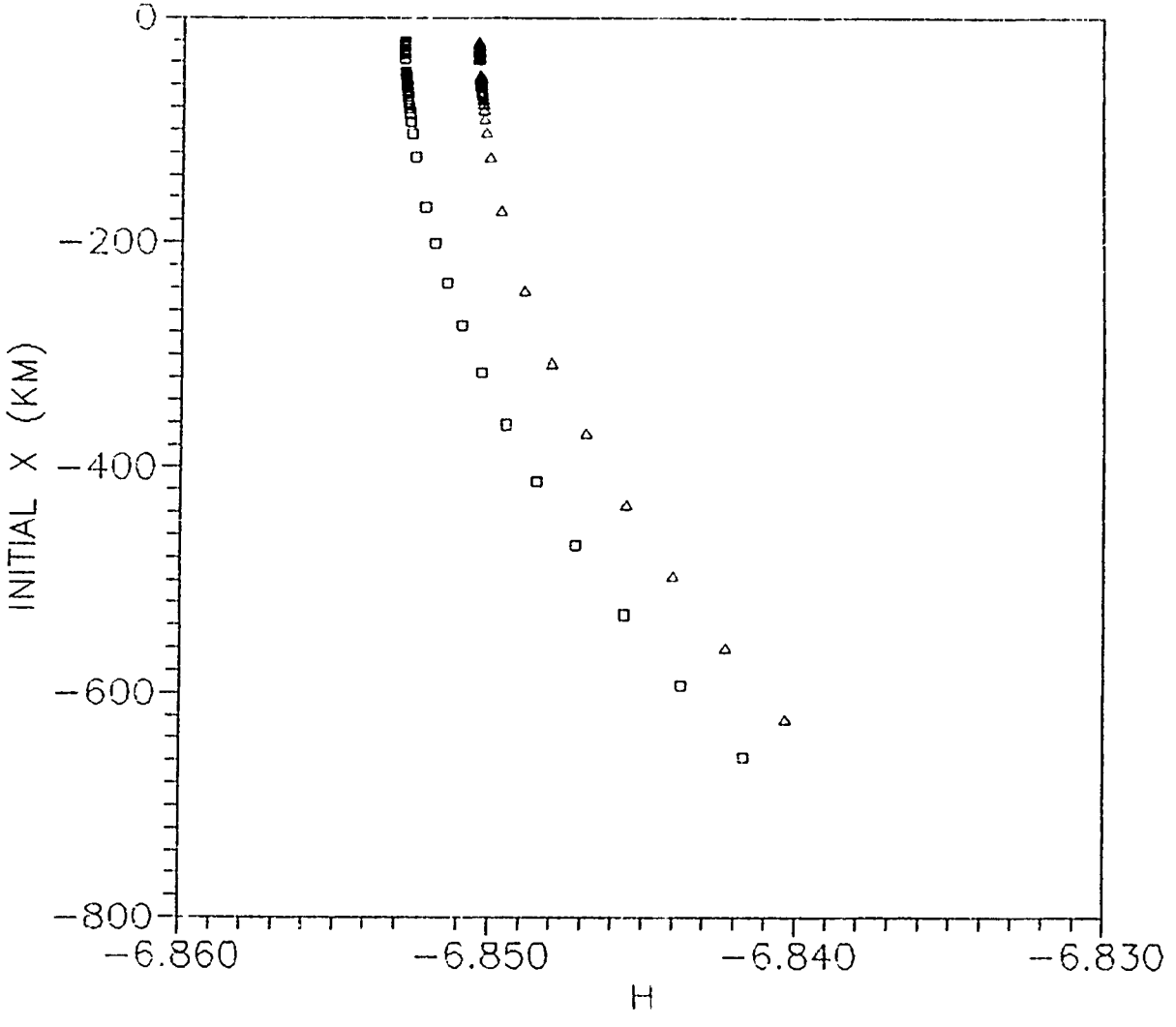

Figure 10. Effects of Correcting Phobos Rotation Rate

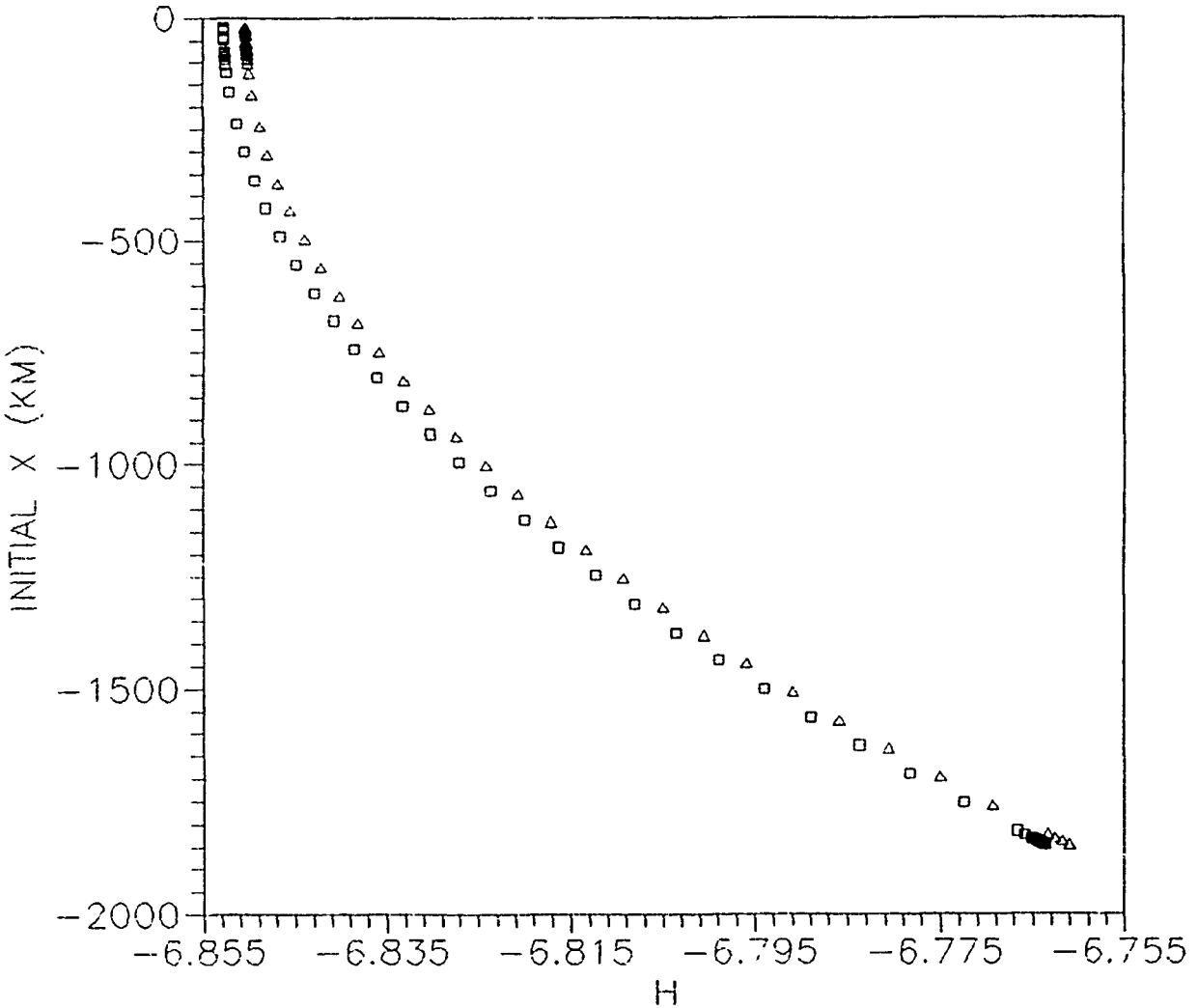

Figure 11. Effects of Correcting Phobos Rotation Rate

Table IV. Stable Centered Orbits Computed About Phobos,
Ω =.00022788 r/s

H	INITIAL X	R_p	R_a	e	PERIOD
-6.85040	-14.2	14.1	16.3	.07	9,538
-6.850399	-17.1	17.0	21.3	.11	12,174
-6.850398	-21.4	21.3	29.8	.17	15,742
-6.850379	-30.2	30.0	49.6	.25	21,123
-6.850361	-40.1	39.9	72.5	.29	24,299
-6.850337	-50.2	50.1	94.9	.31	25,798
-6.850118	-104.7	104.5	207.9	.33	27,364
-6.8500	-124.3	124.1	247.4	.33	27,447
-6.84926	-209.6	209.4	418.8	.33	27,546
-6.84796	-306.9	306.8	613.4	.33	27,564
-6.84522	-446.2	444.7	891.2	.33	27,570
-6.84187	-572.6	571.7	1144.7	.33	27,571
-6.83266	-825.3	825.7	1649.3	.33	27,572
-6.82356	-1014.7	1011.9	2028.0	.33	27,572
-6.81256	-1204.1	1198.4	2404.4	.33	27,573
-6.79593	-1444.1	1443.8	2867.4	.33	27,572
-6.78562	-1600.0	1559.3	3580.6	.39	27,571
-6.76334	-1822.5	1822.0	3603.5	.33	27,572
-6.75889	-1868.0	1866.9	3692.0	.33	27,572

H- Hamiltonian, km^2/s^2
R_p,R_a- Perigee, Apogee Distances, km
e- eccentricity
PERIOD- Period, seconds

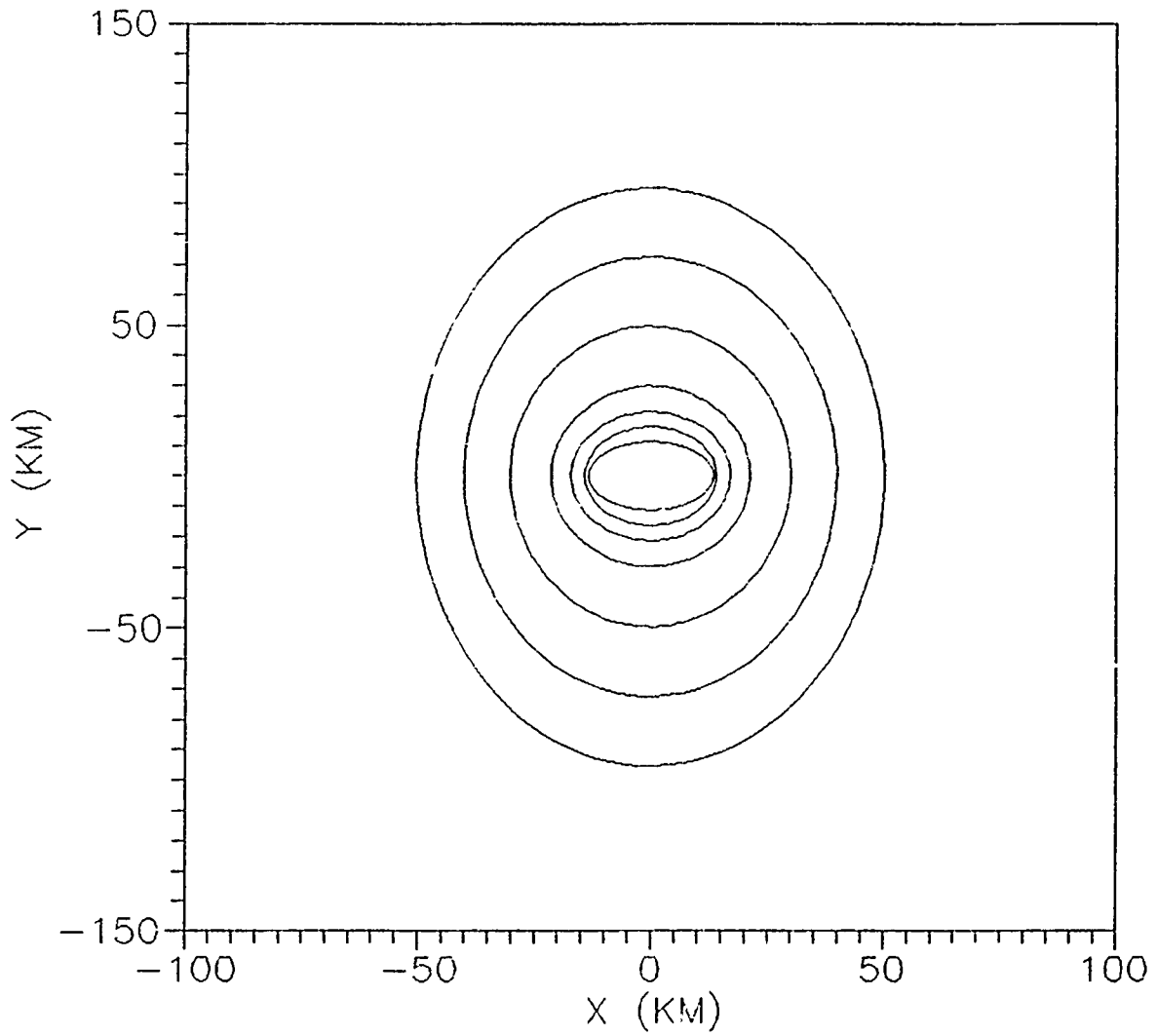

Figure 12. Closest Orbits to Phobos, Ω=.00022788 r/s

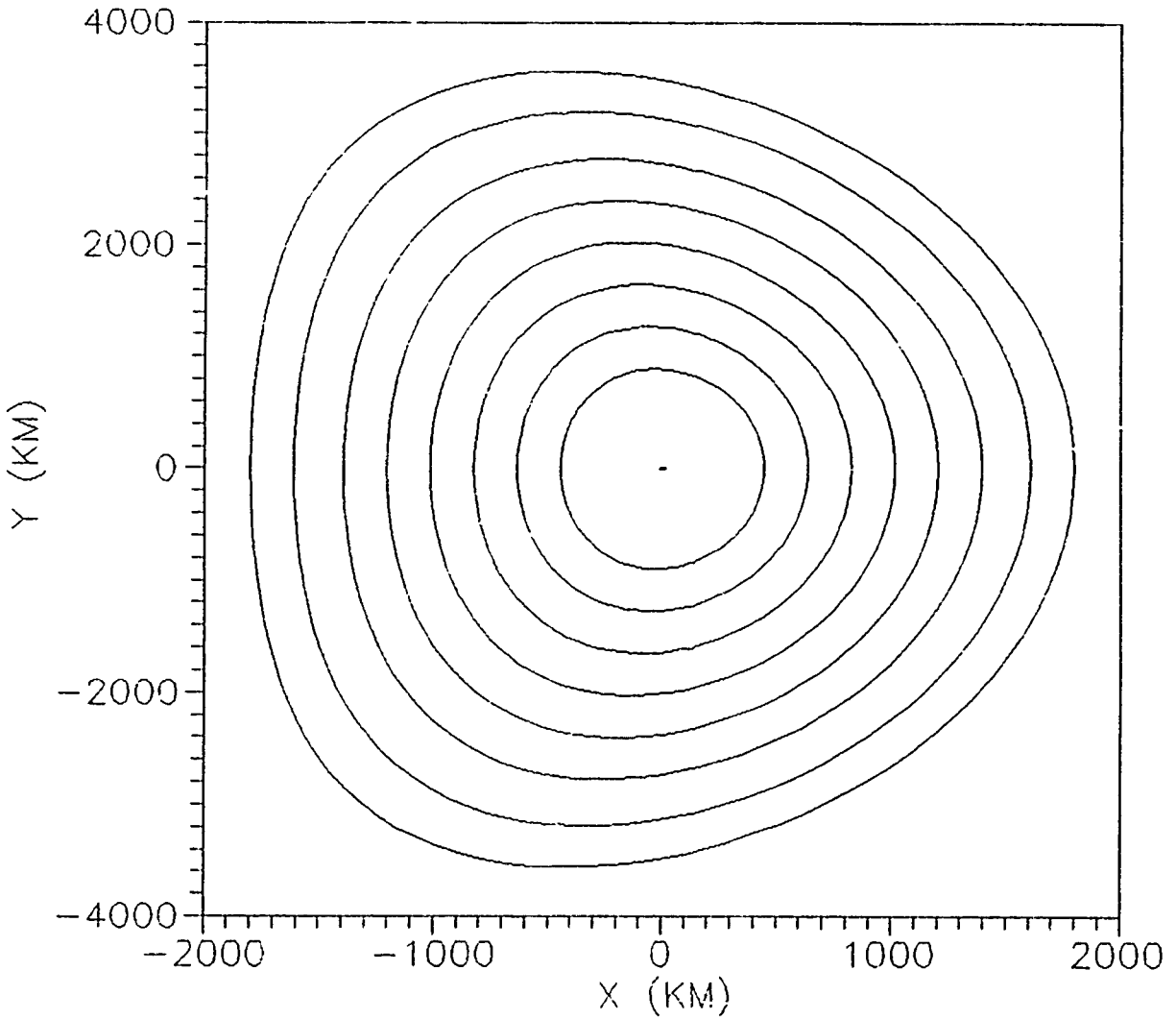

Figure 13. Orbits Furthest from Phobos, Ω=.00022788 r/s

Collision Orbits. Many of the solutions found were orbits that had a perigee point which was inside the surface of Phobos. Other orbits had trajectories completely within the surface of the moon. These orbits are called collision orbits. Figure 14 shows several of these. The continuation run which computed these orbits also found a limit point. This limit point, seen in Figure 15, occurred at parameter value H=-6.850188. From this figure, the solutions are continued with H varying from its initial value of H=-6.850392 at point A. As H decreases, the size of the orbit decreases. This has been the trend in all continuation runs thus far. At point B, H begins to increase again. However, the orbit size continues to decrease, which is unusual. At point C, the Hamiltonian reaches its maximum value then the solutions trace out the path C-D. Point C is a limit point where the solution branch turns around and follows a different path. In no other situation did this occur. This is unfortunate, because all the orbits computed here were collision orbits. Finding limit points while computing larger orbits might have led to discovering different types of orbits, stable or unstable, about Phobos. It was hoped that these collision orbits would "grow" and become realistic orbits of Phobos, perhaps as different types of orbit families. This did not happen.

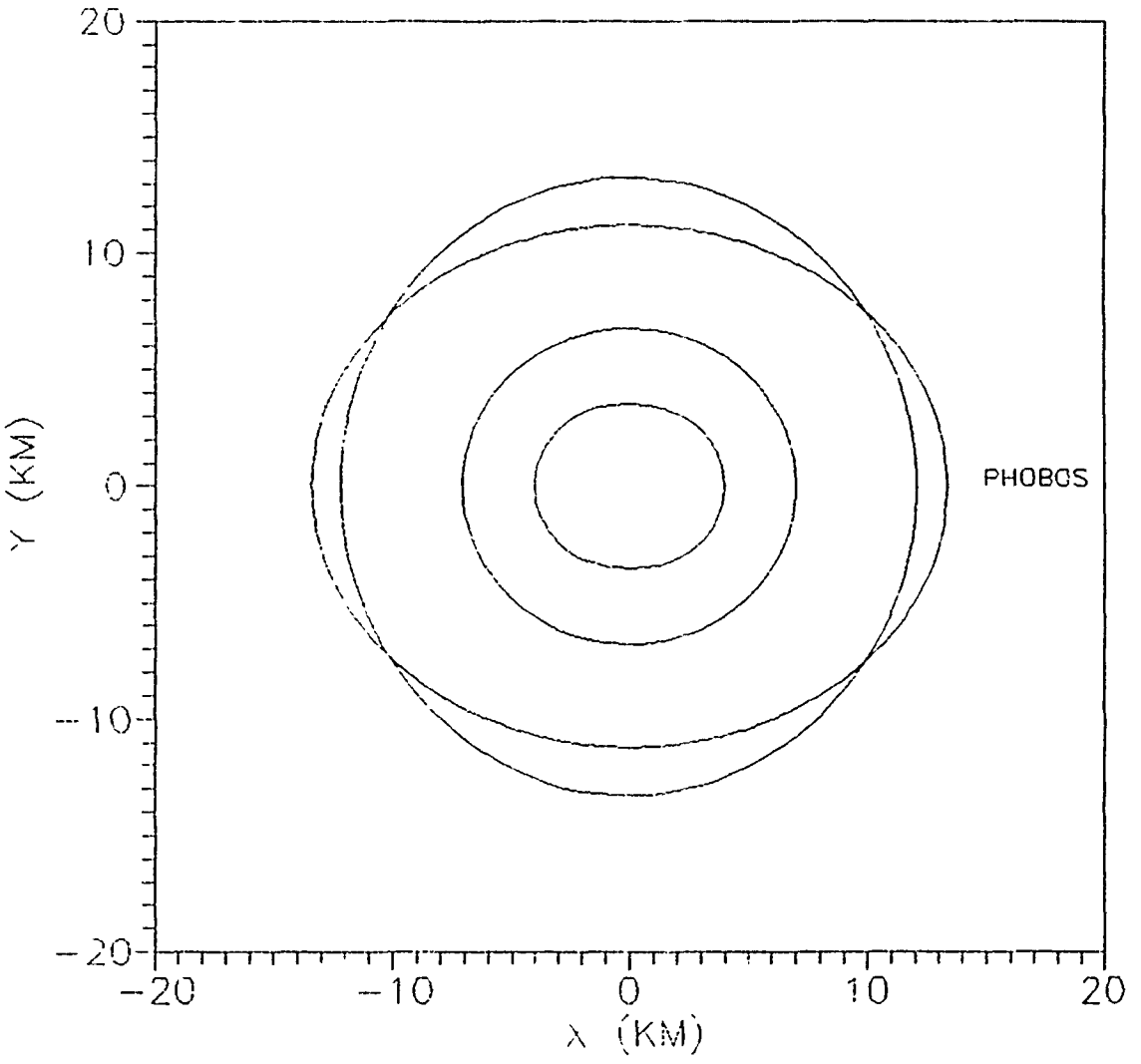

Figure 14. Collision Orbits of Phobos

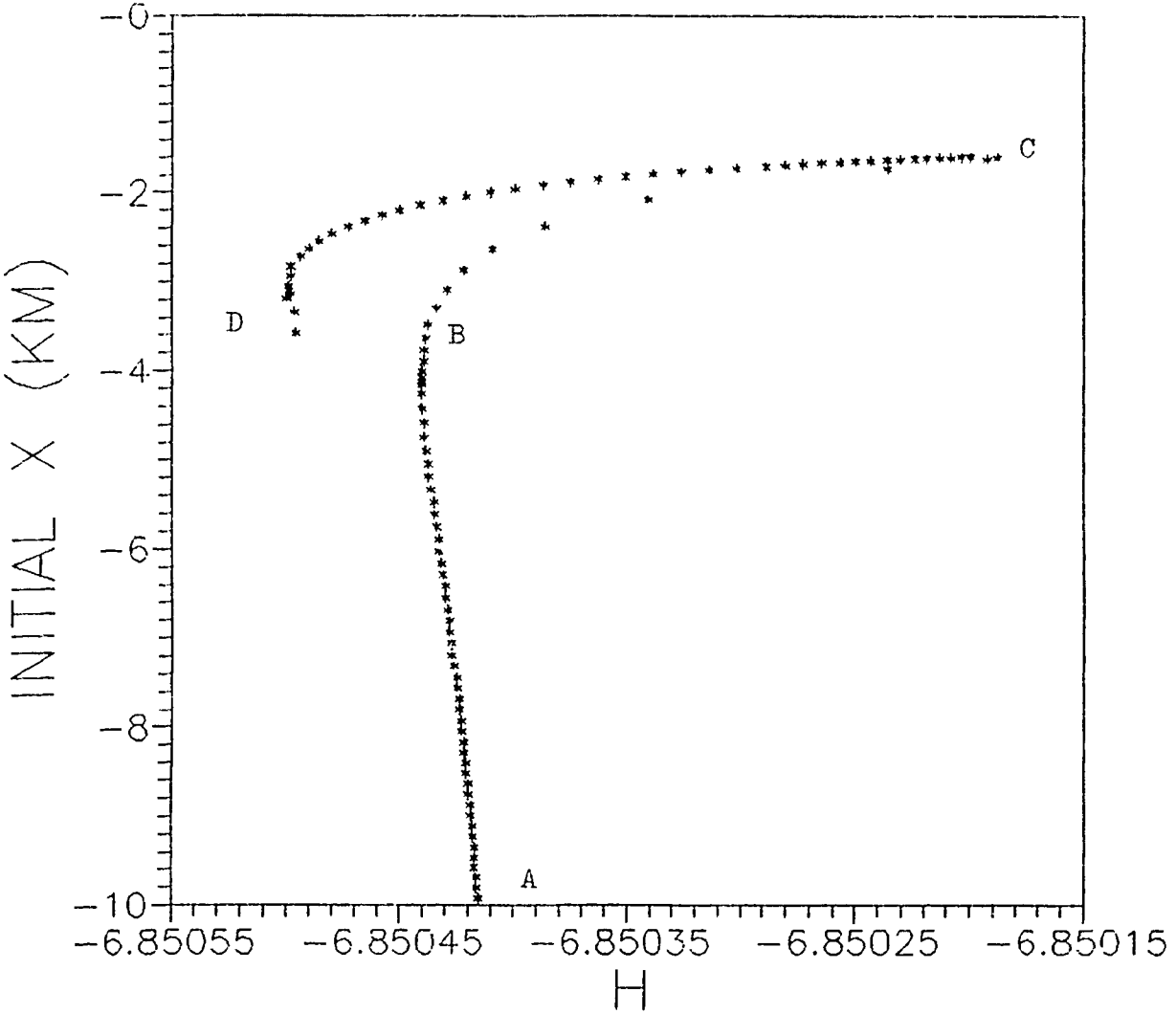

Figure 15. Phobos Limit Point, H=−6.85019

Mass of Phobos Effects. The gravitational parameter of Phobos used in this study is GM_{phob}=.00066 km^3/s^2. This amounts to a mass of 9.9E15 kg. From a recent article in "Sky and Telescope," (3:158) the mass of Phobos was given to be 1.08E17 kg. This is quite a bit larger than the mass used in this study. With this mass, GM_{phob}=.007204 km^3/s^2. Using AUTO, the mass of Phobos was increased and solutions were found. Figure 16 shows that as the gravitational parameter, hence mass is increased, the orbits become larger for the same Hamiltonian value. This makes sense because the larger mass and gravitational parameter cause a decrease in potential energy due to the moon, V_{moon}. This is evident by

$$V_{moon}=-Gm\int\frac{dM_{moon}}{r} \qquad (30)$$

when dM_{moon} is increased. The Hamiltonian is expressed by

$$H=1/2\,(P_x^2+P_y^2)+P_x\Omega Y-P_y\Omega\,(X+D)+V \qquad (31)$$

The smaller V will make the value of H, a negative number, smaller. Therefore, the larger mass of Phobos results in orbits which have a smaller Hamiltonian value for the same size orbit.

Variations In Solutions. Figure 17 shows how the solutions relate to the semi-major axis A. From this, there appears to be places where the solutions are not unique for a value of the Hamiltonian. Figure 18 is an expanded view of the previous figure. At approximately H=-6.8245 and -6.82, it

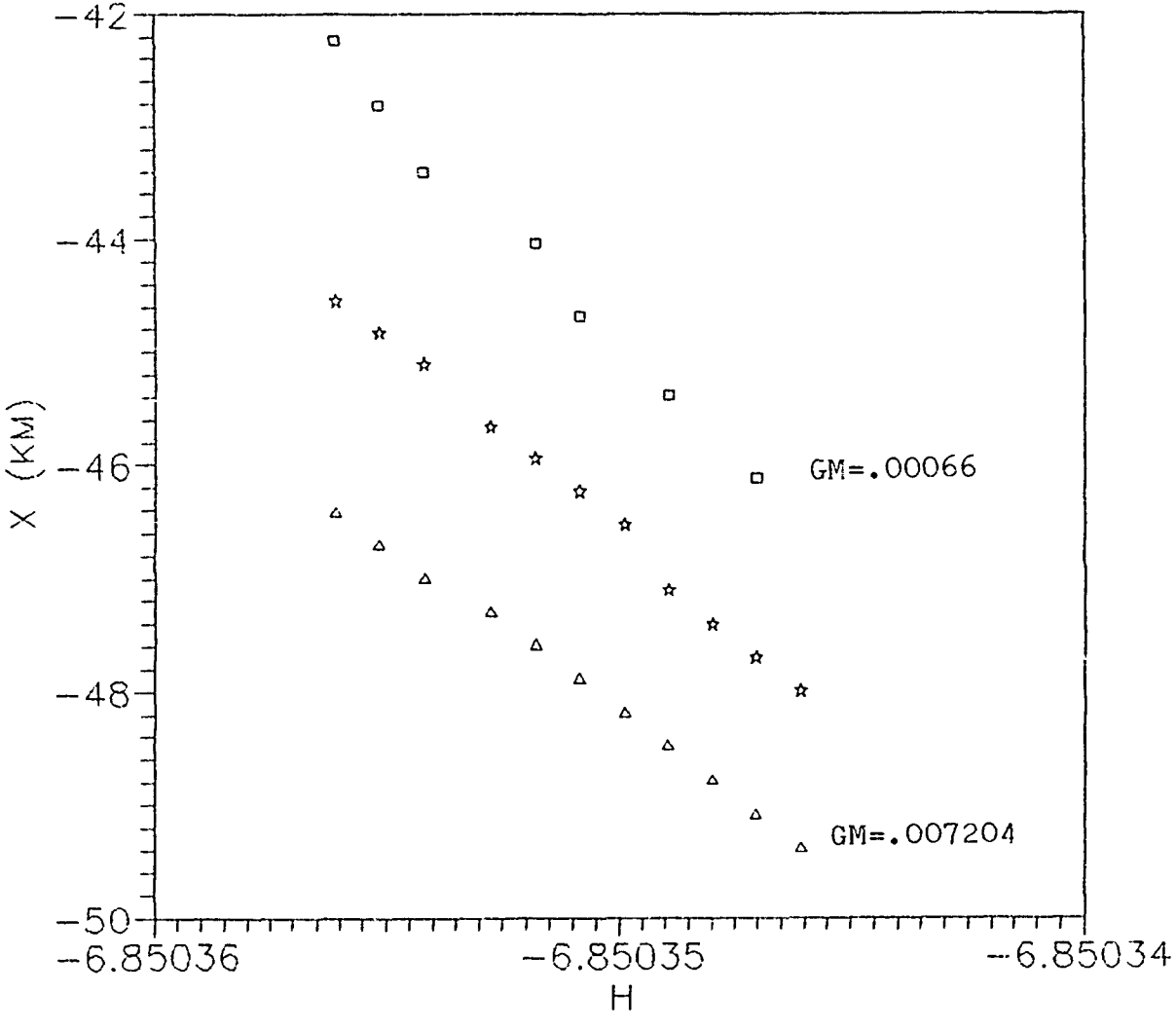

Figure 16. Variations Due to Mass of Phobos

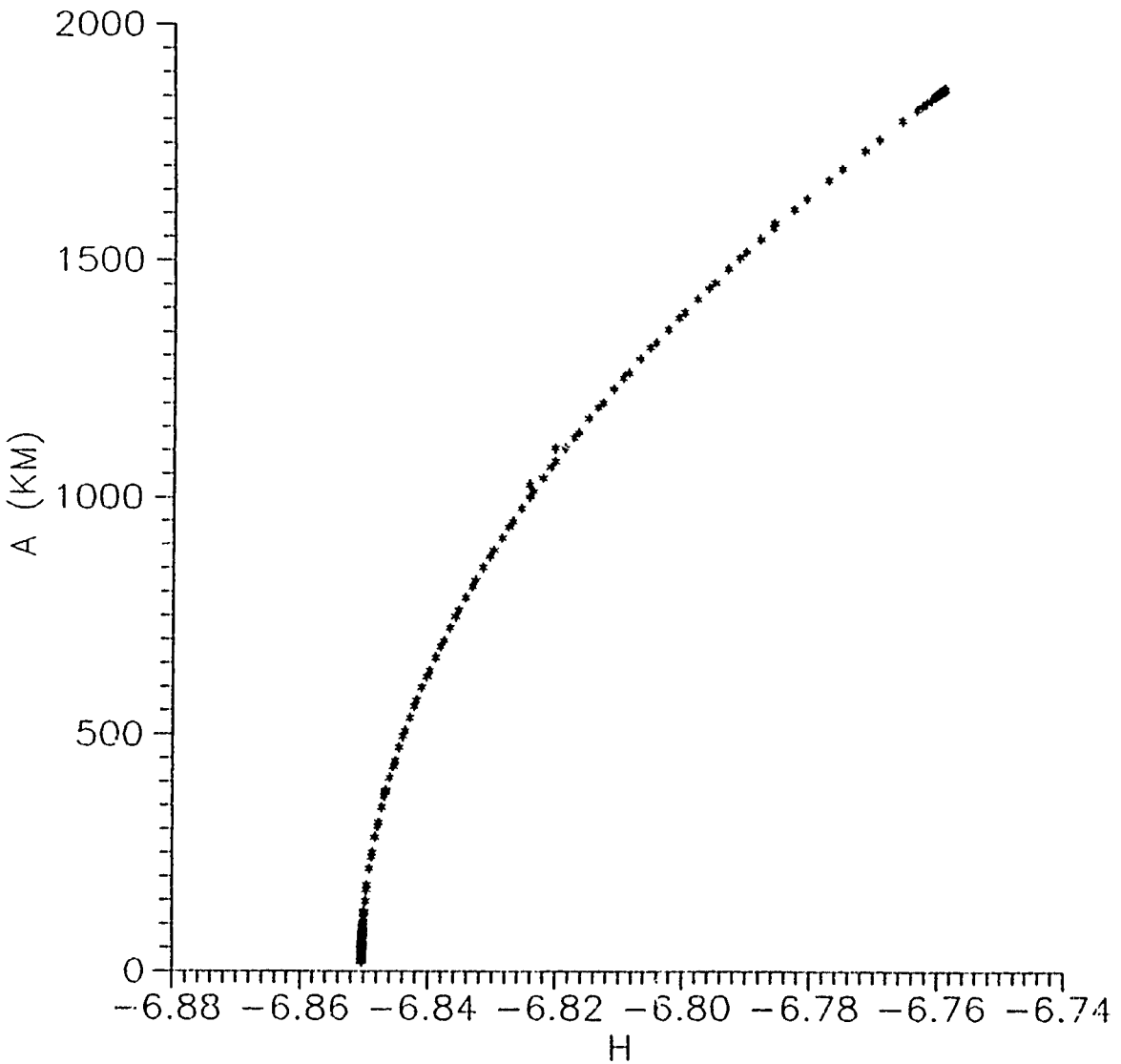

Figure 17. Semi-Major Axis of Phobos Orbits vs H

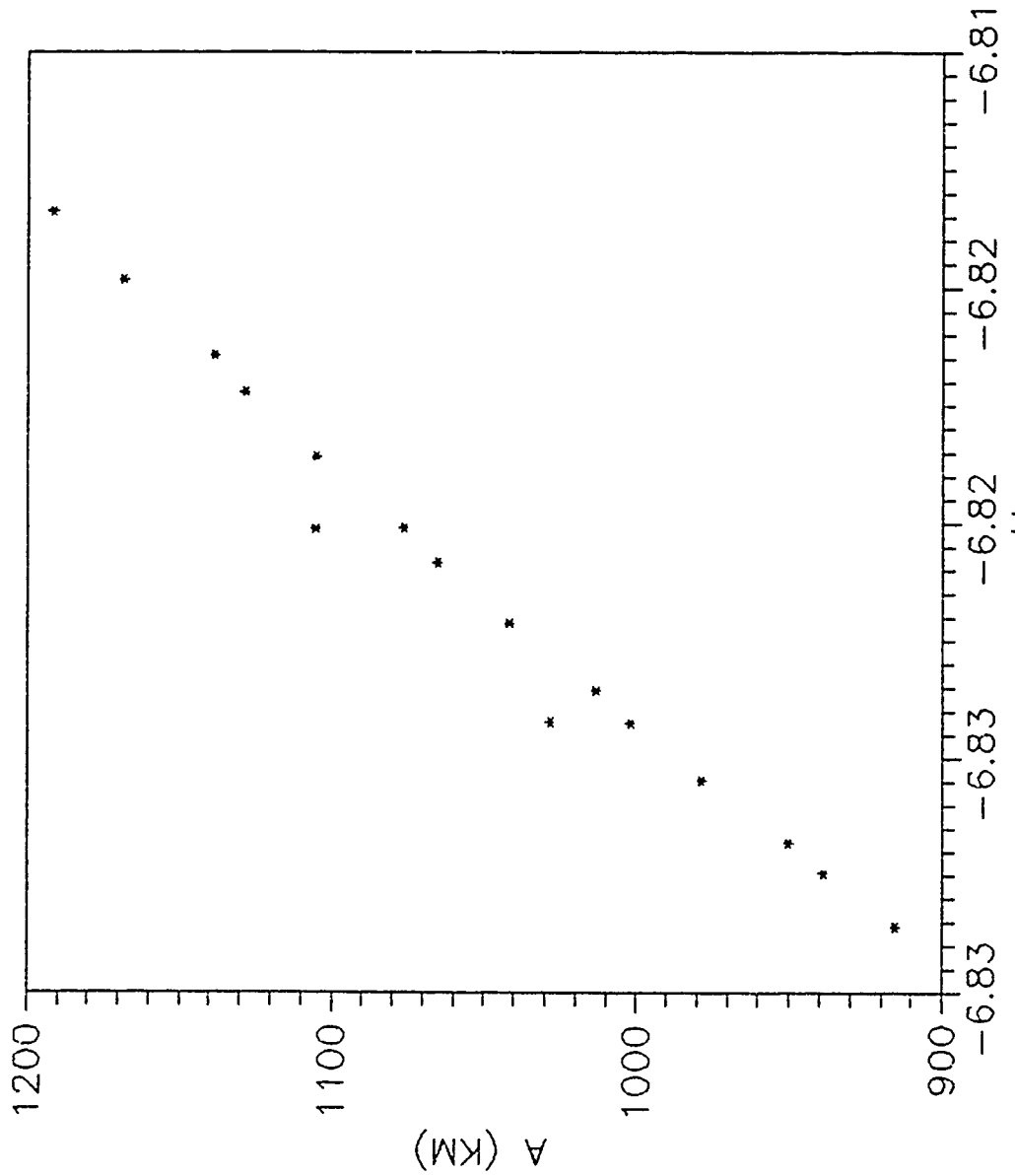

Figure 18. Variations in Solutions for Phobos Orbits

seems that two solutions exist for each value of H. The difference in the size of the semi-major axis in both cases is over 20 km. This shows that the continuation method using AUTO is not perfect. There should be a smoothly increasing or decreasing relationship between the parameter H and the size of periodic orbits computed. In this case and others, this did not occur. Also, many times during the computation of solutions, instead of smoothly varying, the parameter value would "jump around" or frequently change directions. Because of this the output was sometimes hard to follow. The drastic changes could be indications of bifurcations, but as no other solution branches were computed and no bifurcation points indicated, this was discounted.

The separate solutions could be orbits which lie on a torus in the three dimensional subspace corresponding to the $H_0 = H(X,Y,P_x,P_y)$= constant situation.

Stability. As mentioned earlier, AUTO computes the Floquet multipliers for each solution. The number of multipliers on or inside the unit circle is indicated. In the case of periodic solutions, there will be one multiplier on the unit circle at +1; therefore, the location of the others will determine stability. Another multiplier should be inside the unit circle due to the dissipation term. The other two multipliers should be on the unit circle for neutral stability. For a typical continuation run using AUTO, the

multipliers were plotted. The results are shown in Figure 19. Most of the solutions generated multipliers that were on or inside the unit circle. These stable solutions had two multipliers on the real axis, one with a magnitude due to dissipation less than 1 and the other at +1. The other two multipliers were complex conjugate pairs with magnitudes equal to 1. The multiplier shown outside the circle in Figure 19 was associated with the first unstable solution computed for that particular continuation run. From this unstable orbit, which was also a collision orbit, many more unstable orbits were computed.

The behavior of some of these unstable orbits is worth noting. Figure 20 shows a comparison of two orbits computed, both within Phobos, which had the same Hamiltonian value, H=-6.850431. The larger orbit was stable though not realistic and the smaller unstable. Though the smaller orbit was periodic when its trajectory was integrated, its shape was not a simple ellipse, as most orbits computed in this study were. This orbit and several others with the same shape are shown in Figure 21. As the sizes of the orbits in this figure increase, they do not seem to become any more circular. This is expected because of the many nearly circular orbits computed in the proximity of Phobos. The biggest orbit in this figure has the smallest Hamiltonian value, H=-6.850496. No further solutions were computed past this one. It is uncertain

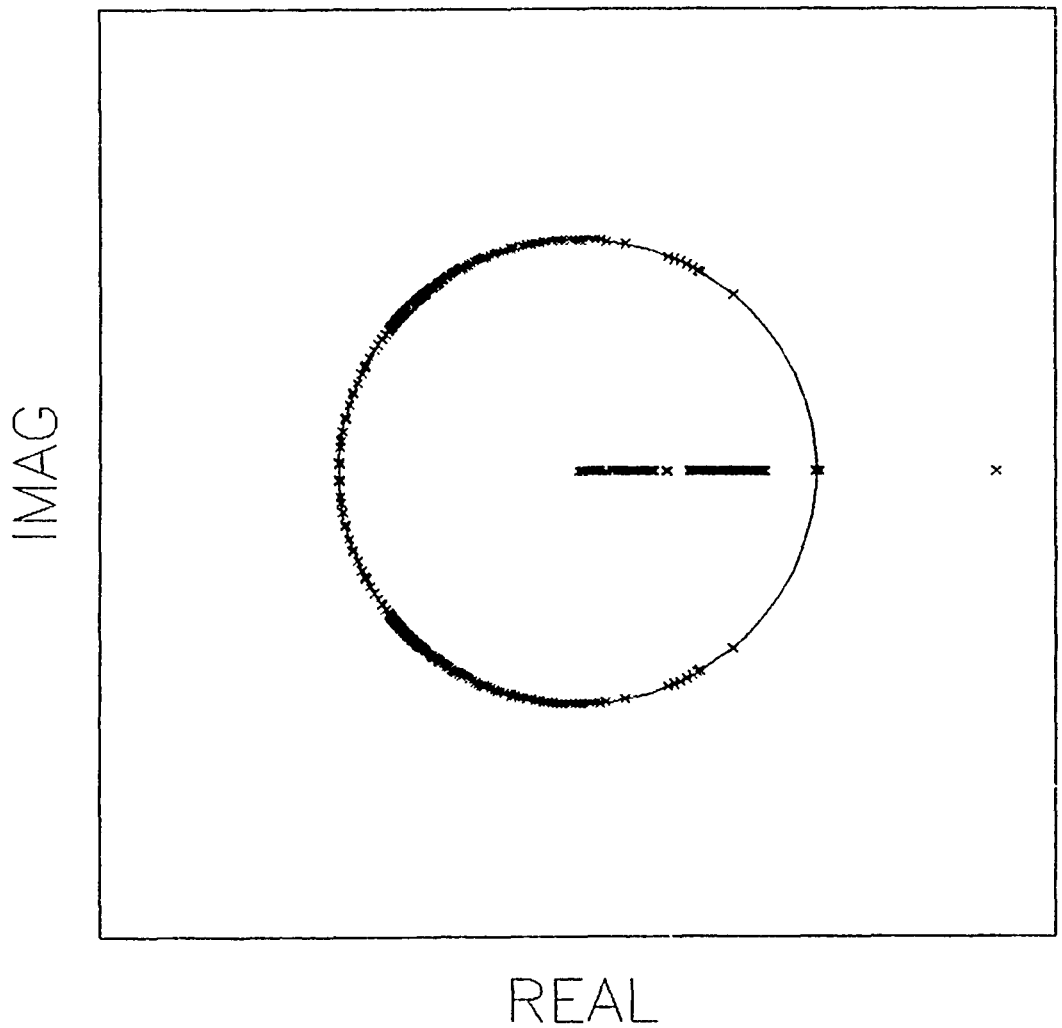

Figure 19. Floquet Multipliers for Phobos Run

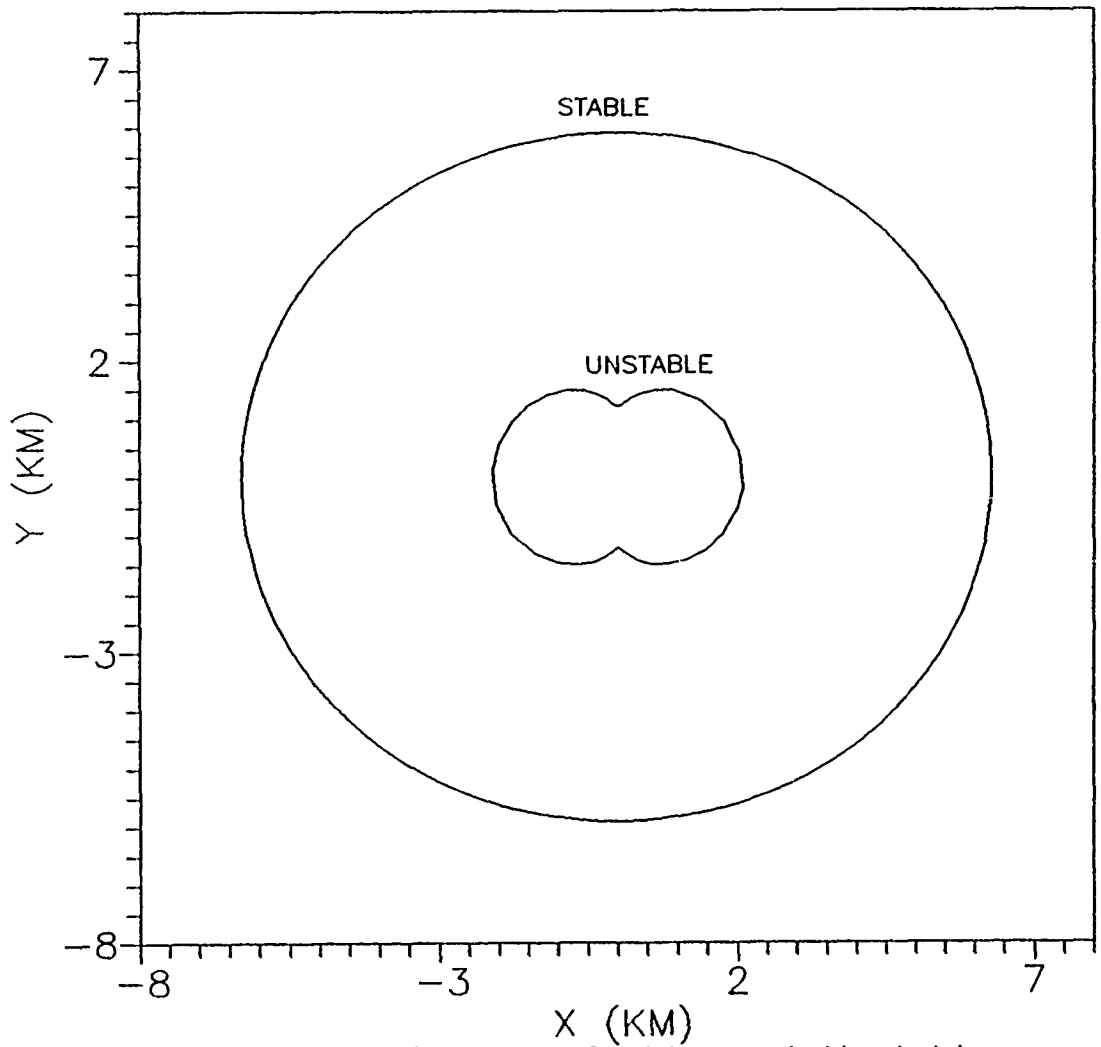

Figure 20. Comparison of Stable and Unstable Phobos Orbits, H=−6.850431

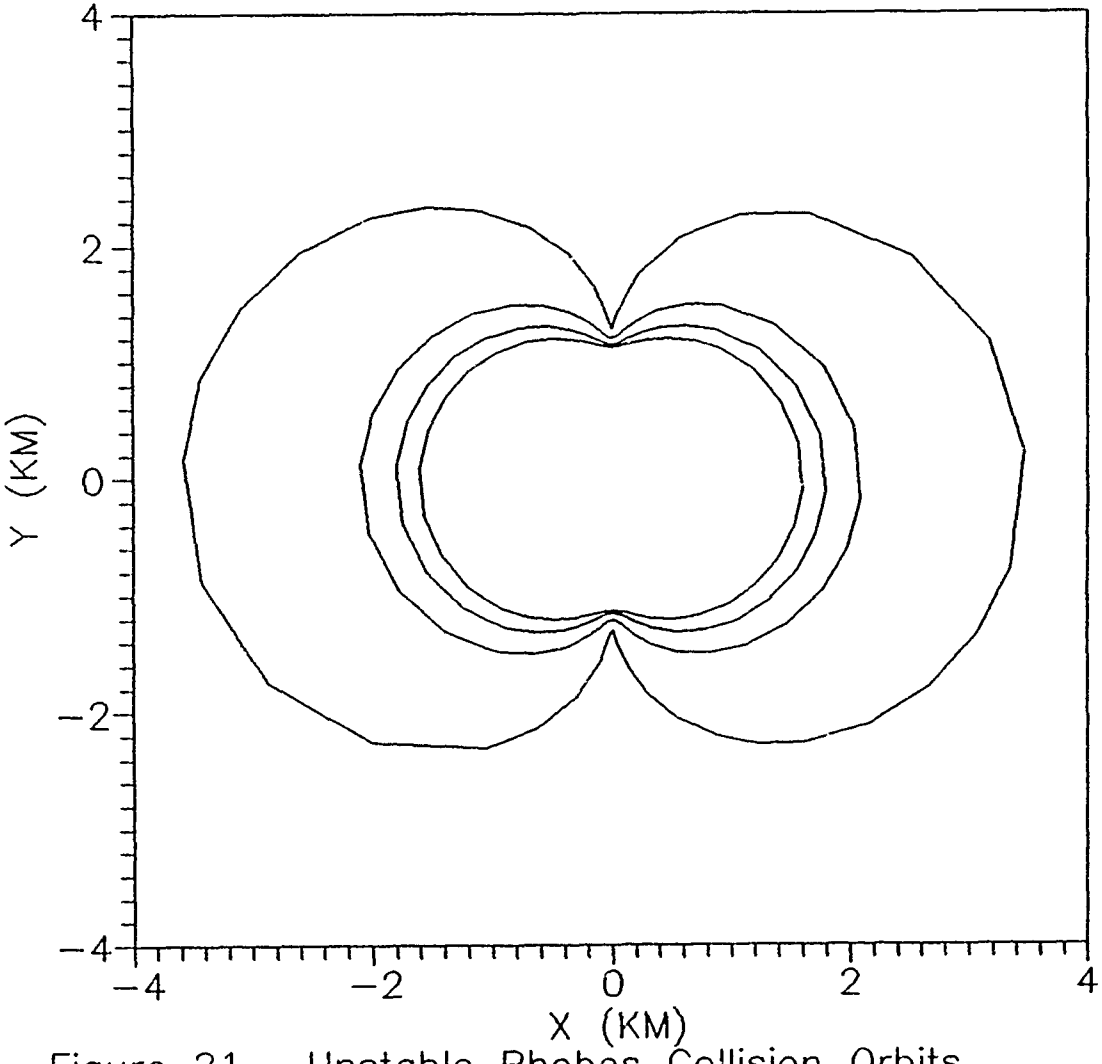

Figure 21. Unstable Phobos Collision Orbits
$H_{min}=-6.850496$

whether the solutions that exist past this orbit become elliptical again or approach infinite period, possibly a heteroclinic orbit. As this behavior occurred in a region of orbits smaller than Phobos, no useful information was gained. It seems clear that a new family of orbits will not "leave" the interior of Phobos.

Deimos

As in the case with Phobos, a continuum of stable orbits were found as the initial Hamiltonian value was varied.

Stable Orbit Verification. Table V contains a summary of the orbits computed. Again, this is a summary of many more stable orbits that were computed. As with Phobos, the period of these orbits increased with an increasing Hamiltonian value until the period of Deimos was reached, approximately 109,000 seconds. These orbits had periapsis distances that ranged from just above the surface of Deimos to 4100 km, which is over one-sixth the distance to Mars. Figure 22 compares the initial x-values of these orbits with the ones previously found. Both sets of solutions are in agreement. These orbits were again retrograde (clockwise) with respect to the rotation of Deimos. It was also noticed from the complete set of solutions computed, that the sizes of the orbits increased less and less for the same increase in Hamiltonian value.

Complete Solutions. The low altitude orbits, shown in Figure 23, are not the rotating ellipse type found in pre-

Table V. Stable Orbits About Deimos

H	INITIAL X	R_p	R_a	e	PERIOD
-2.738593	-8.21	7.83	8.02	.01	11,000
-2.738593	-8.75	8.33	8.58	.01	14,172
-2.738593	-9.38	8.91	9.29	.02	15,648
-2.738592	-10.03	9.49	10.01	.03	17,204
-2.738592	-10.69	10.11	10.76	.03	18,800
-2.738590	-20.09	19.11	23.80	.11	43,325
-2.738588	-30.42	29.23	43.81	.20	68,583
-2.738585	-50.10	48.75	88.82	.29	95,051
-2.738570	-109.30	107.81	214.60	.33	107,554
-2.738522	-202.42	200.90	402.62	.33	108,842
-2.738309	-411.67	410.16	821.94	.33	109,055
-2.737991	-601.04	599.84	1200.98	.33	109,074
-2.736828	-1030.19	1028.59	2059.00	.33	109,081
-2.736120	-1219.76	1218.97	2439.11	.33	109,083
-2.734672	-1535.71	1533.63	3072.72	.33	109,084
-2.733644	-1725.24	1724.08	3452.79	.33	109,085
-2.731663	-2041.06	2037.37	4081.47	.33	109,086
-2.727798	-2546.09	2536.66	5083.73	.33	109,090
-2.723074	-3050.70	3036.71	6087.03	.33	109,096
-2.710174	-4120.24	4107.76	8198.09	.33	109,129

H- Hamiltonian, km^2/s^2

R_p, R_a- Pericenter, Apocenter Distances, km

e- eccentricity

PERIOD- Period, seconds

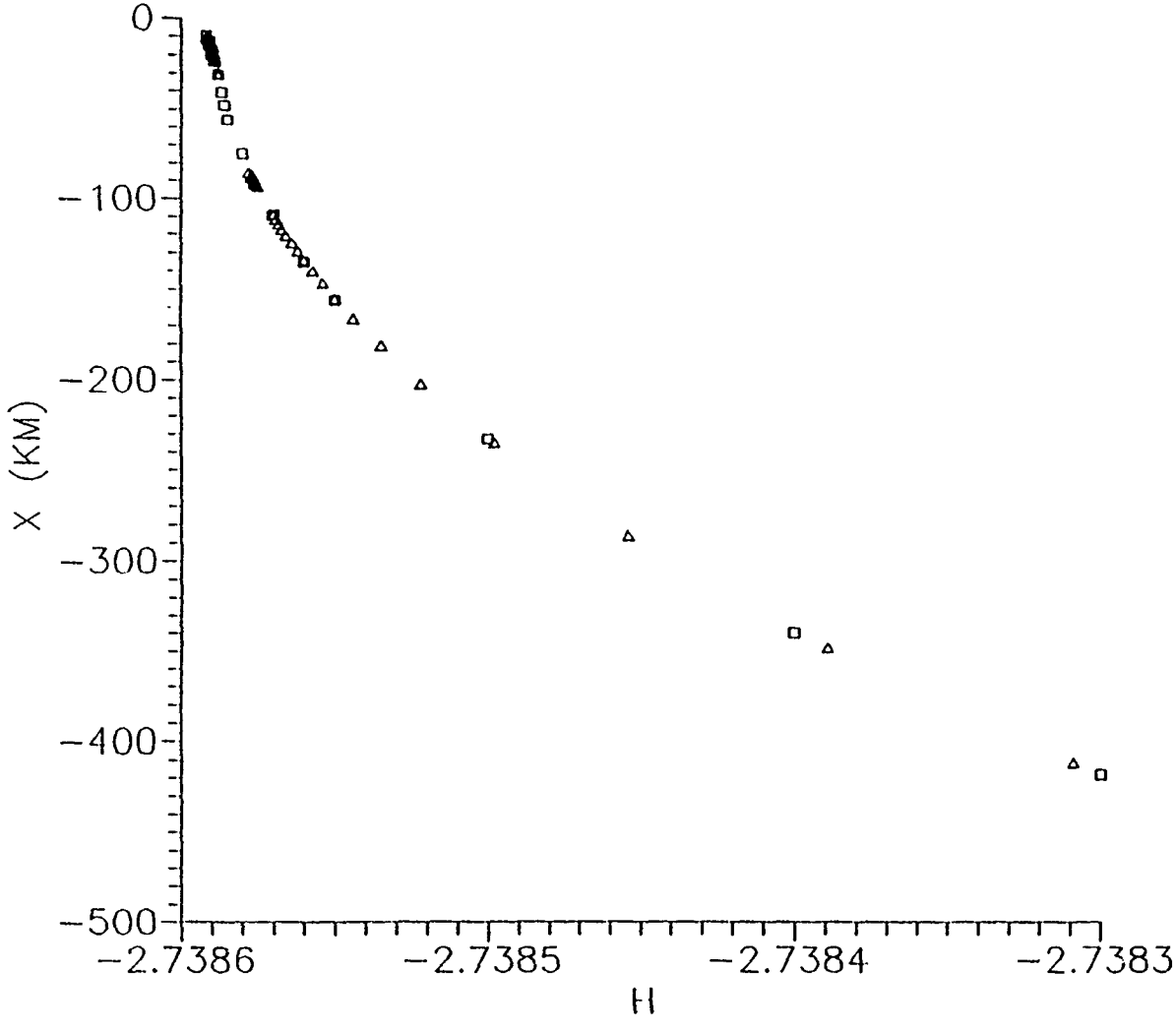

Figure 22. Comparison of Computed vs Previous Orbits for Deimos

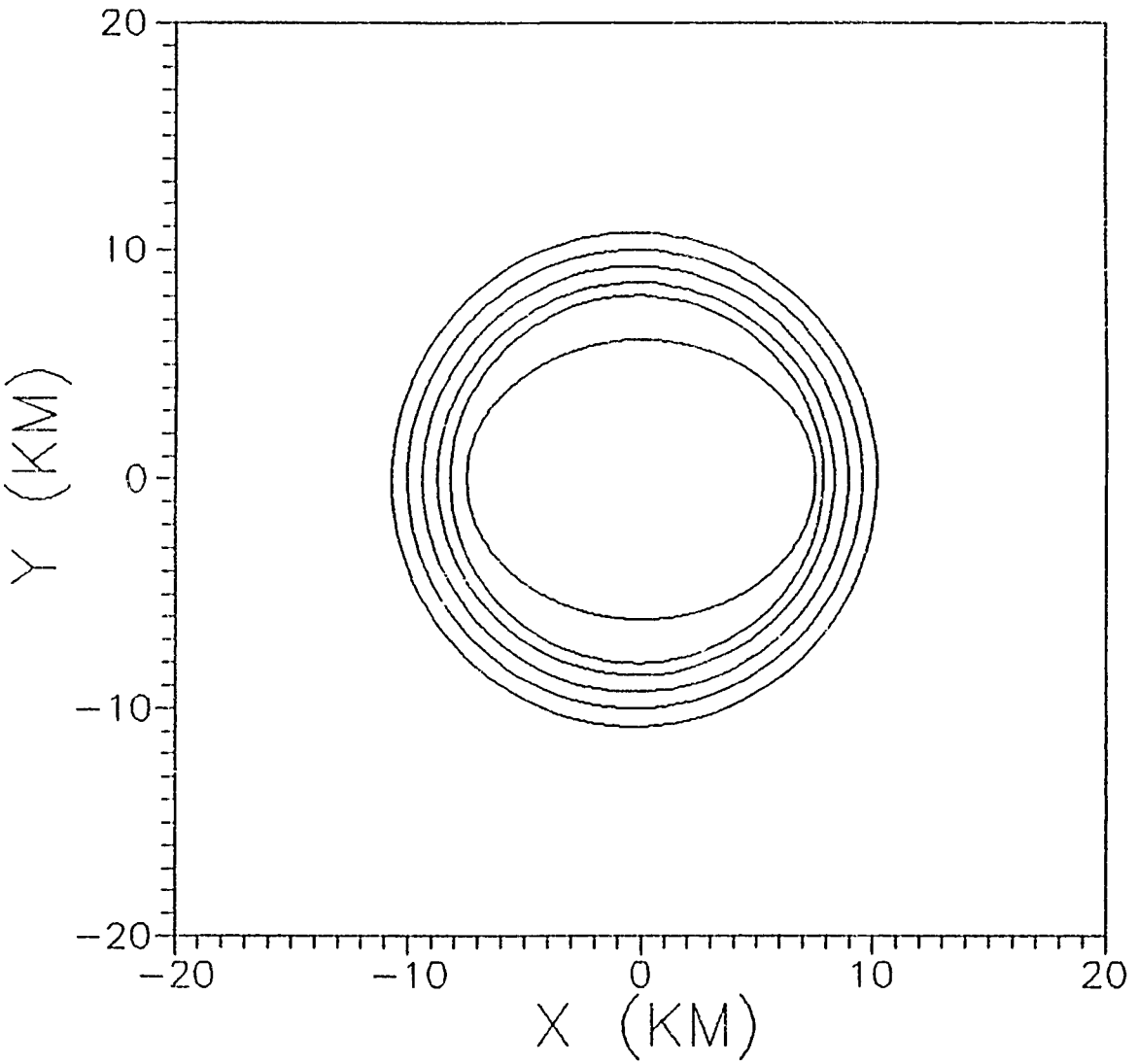

Figure 23. Orbits Closest to Deimos

vious work. In the case of the rotating ellipse discovered, the apogee and perigee locations changed with each satellite revolution and traced out a nearly circular path about Deimos (4:51-54). The low altitude orbits shown in Figure 23 are non-rotating simple periodic orbits, the same type found in the Phobos analysis.

As seen in Table V, these low altitude orbits are nearly circular, having very small eccentricities. However, as the orbits increase in size, they get less circular and converge to an eccentricity of about .33. This follows the pattern of the orbits about Phobos, which were nearly circular close to the surface and became less circular to an eccentricity value of .33. As the satellites move further away from their respective moons, they settle into elliptical orbits about Mars. In both cases, the orbits became similar in shape, with eccentricities of .33. But the largest Deimos orbits computed were over twice as far from their moon as the largest Phobos orbits. These orbits can be seen in Figure 24.

Collision Orbits. Many of the computed orbits had a periapsis point which was inside the surface of Deimos. Several of these collison orbits are shown in Figure 25. The interesting case found with Phobos, where different size orbits were discovered for the same Hamiltonian value did not occur with Deimos. No limit points were computed.

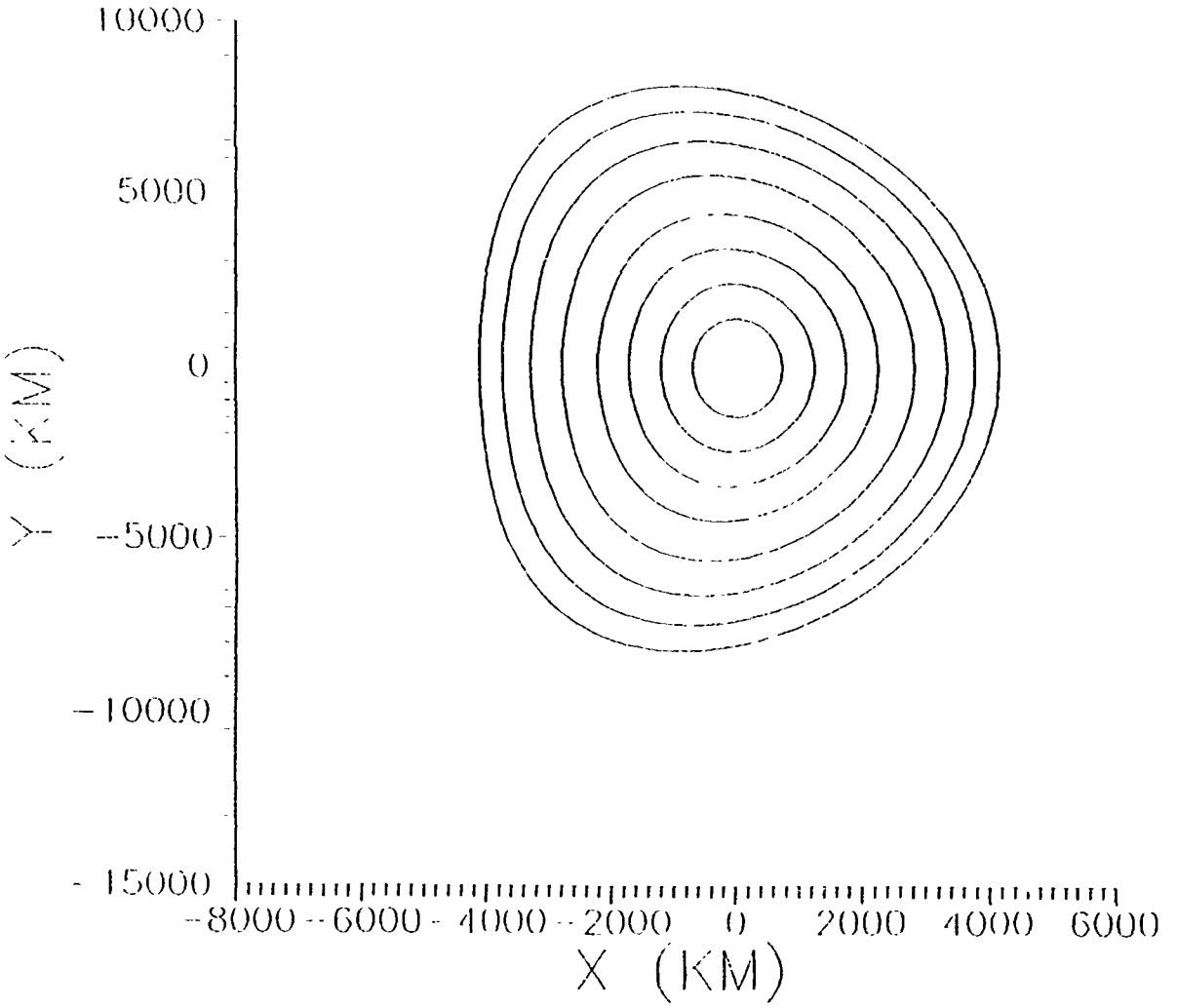

Figure 24. Orbits Furthest from Deimos

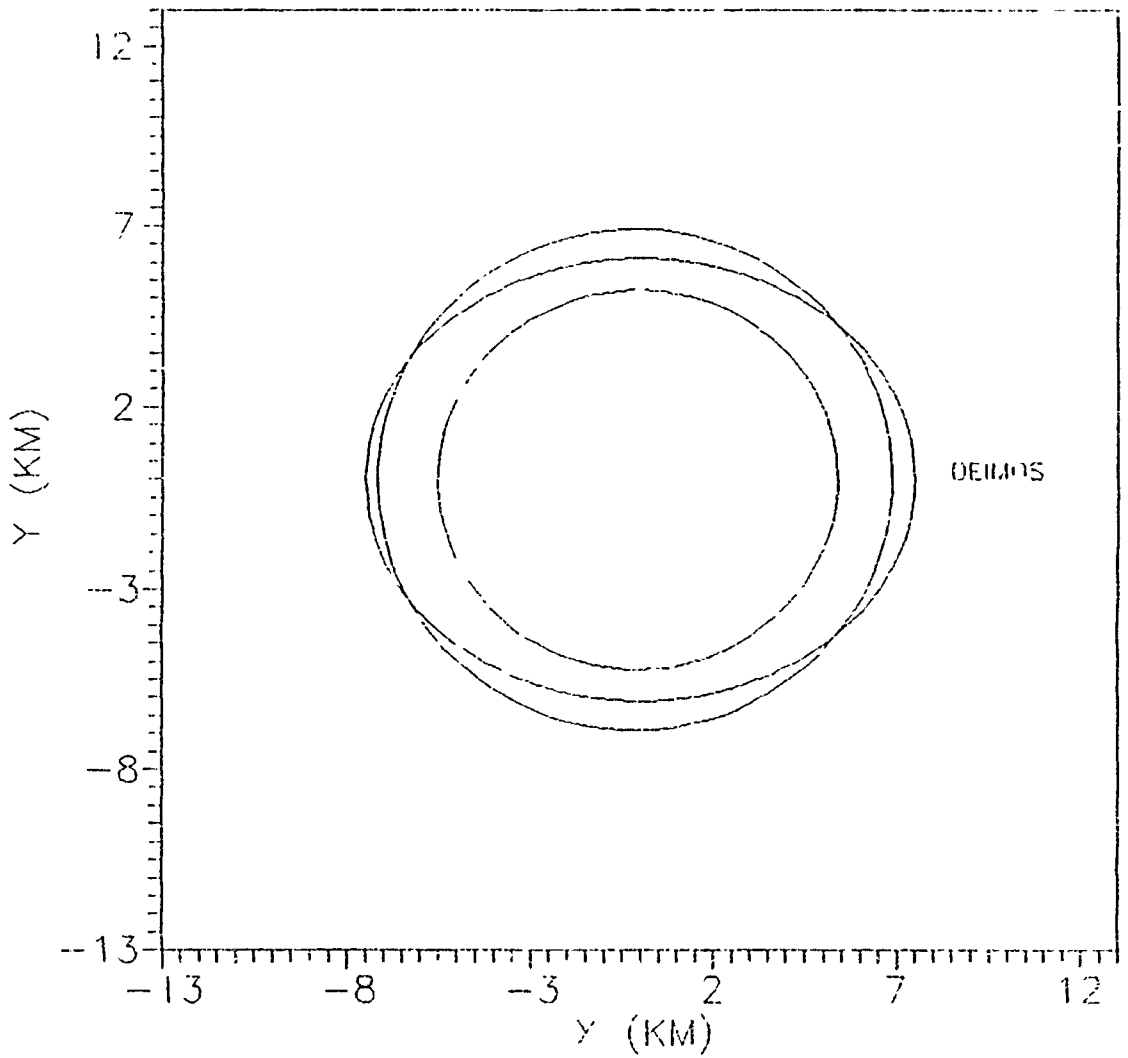

Figure 25. Collision Orbits of Deimos

Stability. The orbits computed for Deimos, summarized in Table V, were stable. Again, their Floquet multipliers were computed and the three not affected by the dissipation term were found to be on the unit circle. For a typical continuation run of solutions, Figure 26 plots the multipliers in relation to the unit circle.

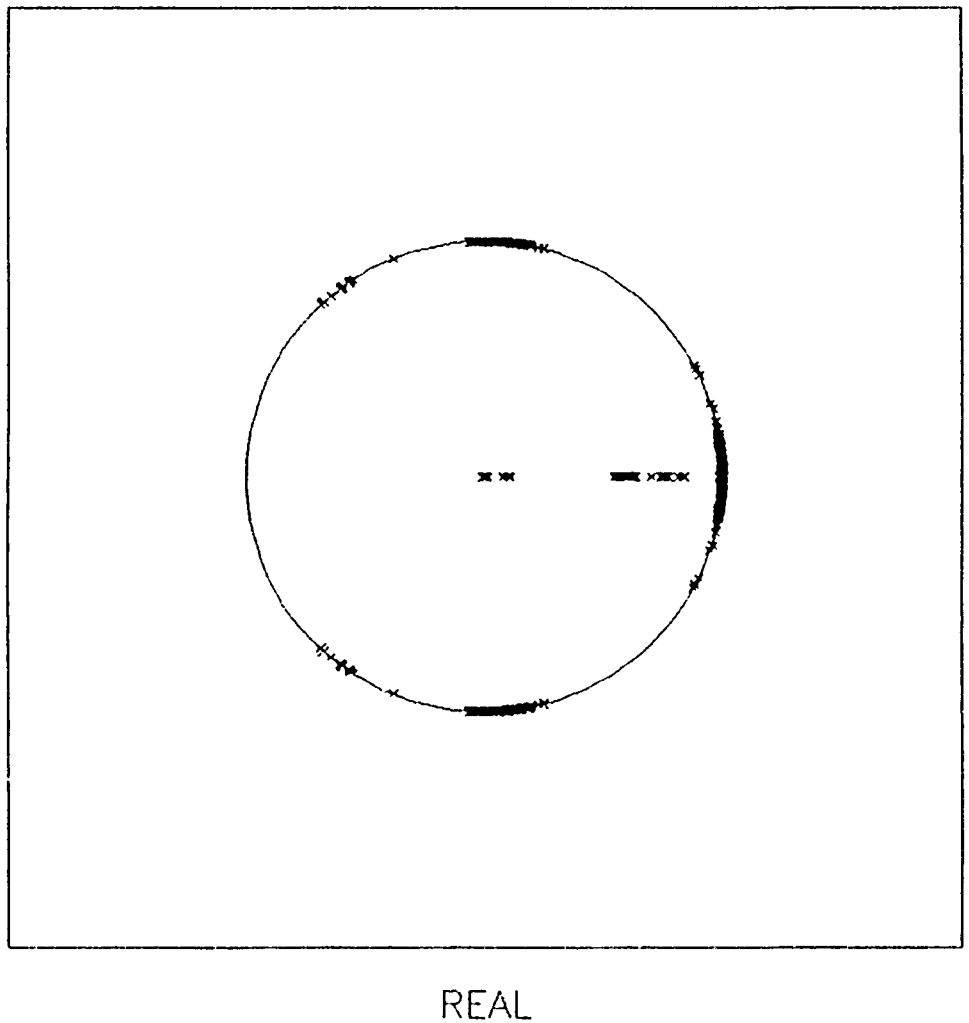

Figure 26. Floquet Multipliers for Deimos Solutions

VI. Conclusions and Recommendations

Using previously found periodic orbits of Phobos and Deimos enabled many more to be found using the continuation techniques discussed in this study. The orbits computed that were closest to the surfaces of the moons were associated with the smallest Hamiltonian values and the largest orbits had the largest Hamiltonians. The orbits closest to the moons seem to be perturbed the most, having short periods and low eccentricities. As the distances increased, the orbits tended to become eccentric, $e \approx .33$, and settle into Martian orbits, with the same periods as their respective moons. These results agreed with previous work.

The search for different branches of solutions and limit points was disappointing, only one was found in the Phobos case. The discovery of more of these could have lead to different types of orbits, possibly prograde instead of retrograde or possibly more resonant orbits. Some unusually shaped orbits were computed, but did not lend themselves to further analysis being very unstable and not in the range of possible orbits about Phobos.

The continuation/bifurcation software AUTO was of limited utility in this type of problem. It was used to find a wide range of orbits, but for this study was not very effective in finding branch points associated with nonlinear behavior. For this modified three body problem there is no naturally

was added to enable AUTO to compute periodic solutions. This introduced energy dissipation, which is characteristic of the nonconservative systems upon which AUTO is primarily used.

This technique did allow various system parameters to be changed and resulting orbital behavior analyzed. The mass of Phobos was increased to show that this causes orbits with the same Hamiltonian value to increase in size. Also, the rotation rate of Phobos was decreased to show that this tended to shift the stable orbits over the center of Phobos and decrease their size for the same parameter, H, value.

The way this system was modeled, utilizing the equations of motion in Section III, AUTO was used stricly as a continuation tool to find more of the same types of solutions. Its capability to find bifurcations and describe nonlinear system behavior was not effective. Perhaps with a system having more parameters, or a nonconservative system where the Hamiltonian would vary on the trajectory, AUTO would be more useful in mapping out the behavior of solution branches and locating branch points.

Appendix A: System Parameters (4:67)

Moons:	Phobos	Deimos
Axis Lengths (km)		
	x= 13.4	x= 7.5
	y= 11.2	y= 6.1
	z= 9.2	z= 5.2
Moments of Inertia ($kg*km^2$)		
	$I_{xx}= 42.016*M_{moon}$	$I_{xx}= 12.850*M_{moon}$
	$I_{yy}= 52.840*M_{moon}$	$I_{yy}= 16.658*M_{moon}$
	$I_{zz}= 61.000*M_{moon}$	$I_{zz}= 18.692*M_{moon}$
Density (g/cm^3)		
	$\mu = 2.2$	$\mu = 1.7$
Orbital Radius (km)		
	D= 9,378	D= 23,459
Rotation Rate (rad/sec)		
	$\Omega = 2.2788*10^{-4}$	$\Omega = 5.76*10^{-5}$
Gravitational Attraction (km^3/sec^2)		
	$GM_{moon}= 6.6*10^{-4}$	$GM_{moon}= 8.8*10^{-5}$

Mars:

Gravitational Attraction (km^3/sec^2)

$GM_{mars}= 42828.32$

Appendix B: Phobos Resonant Orbit Plots

Figure Page

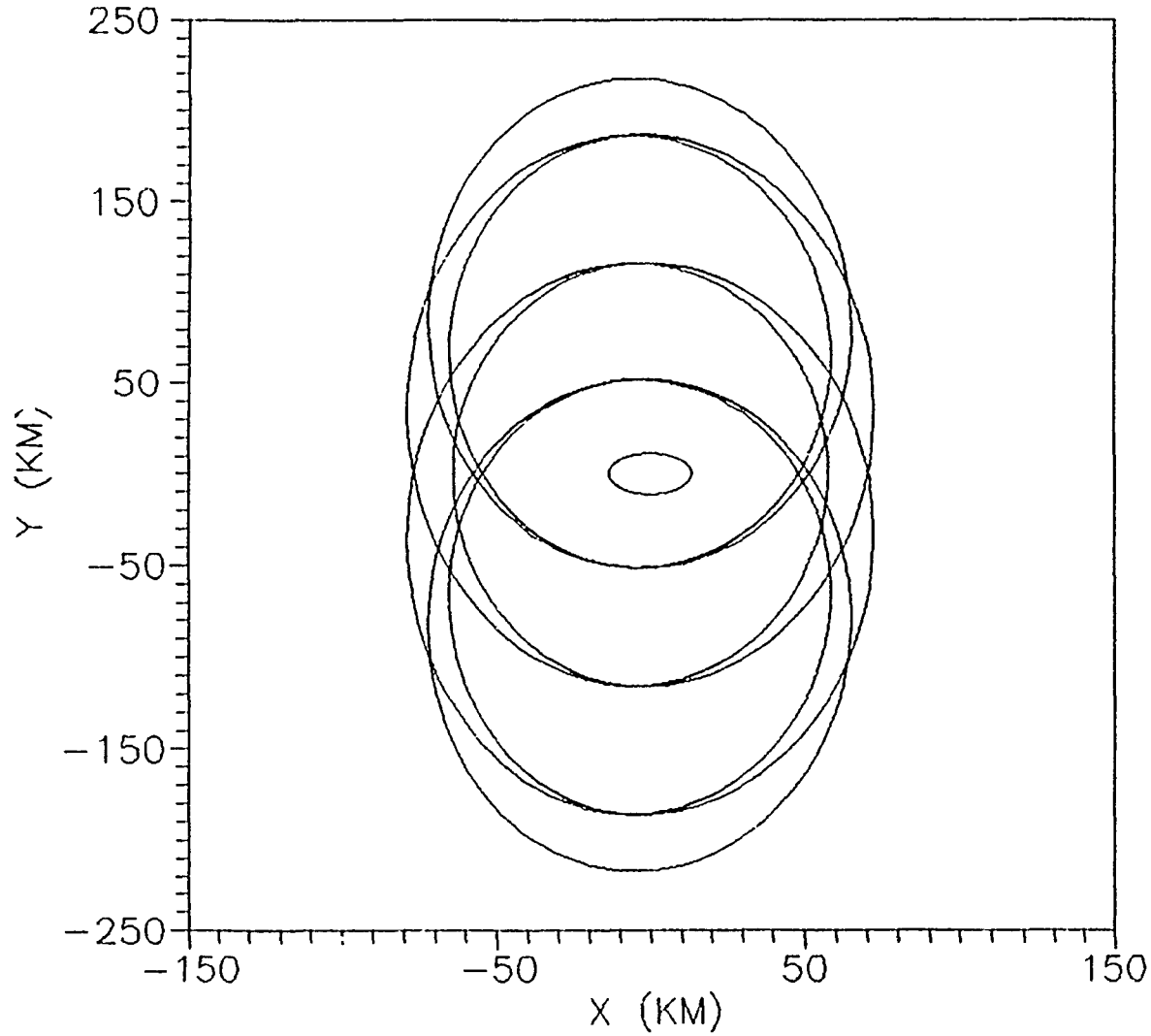

Figure 27. Phobos Resonant Orbit, H= −6.852687

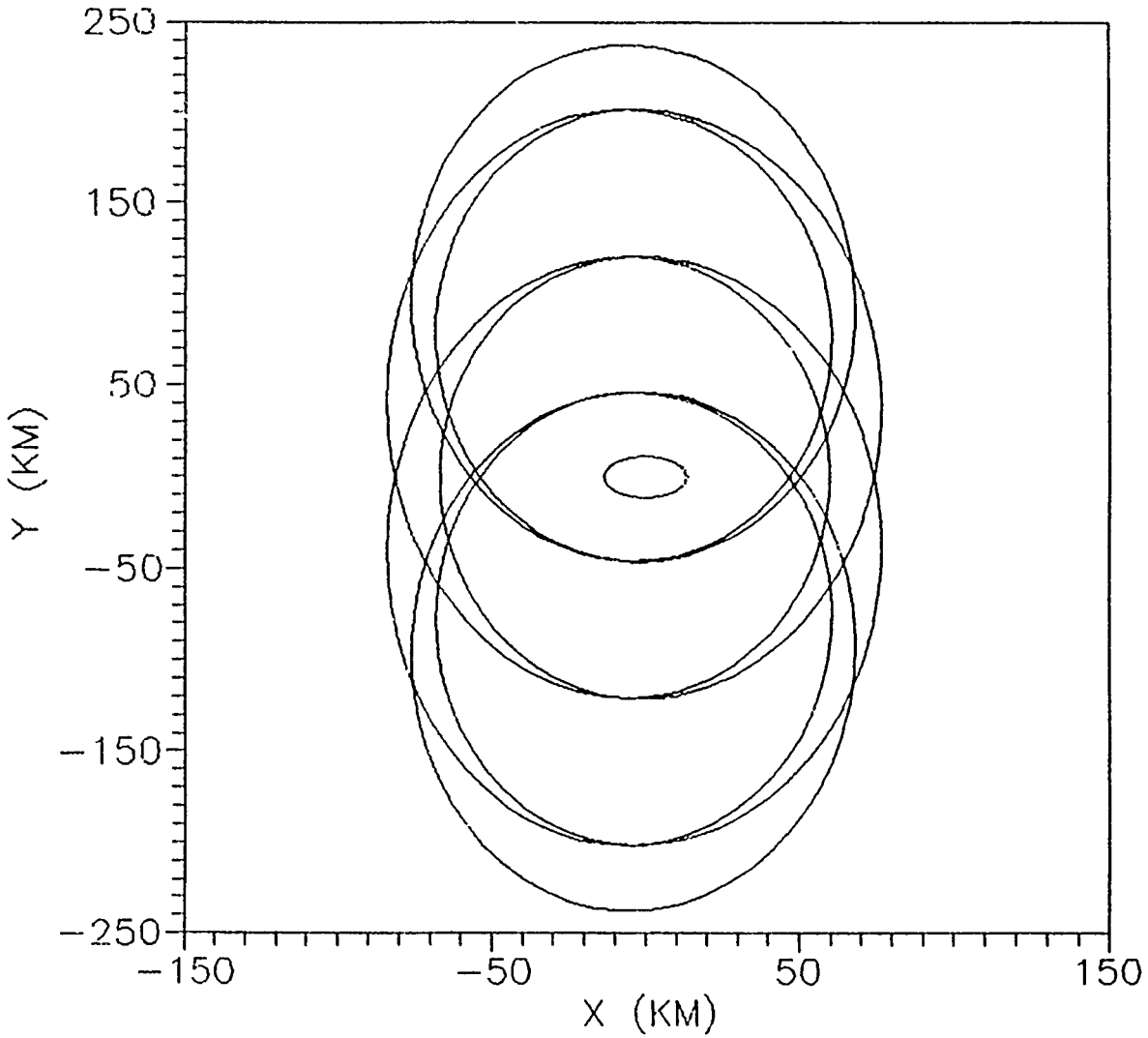

Figure 28. Phobos Resonant Orbit, H= −6.852674

Bibliography

1. Baker, Christopher T.H. and Chris Phillips. The Numerical Solution of Nonlinear Problems. New York: Oxford University Press, 1981.

2. Doedel, Eusebius J. AUTO: Software for Continuation and Bifurcation Problems in Ordinary Differential Equations. Soft-ware Users Manual, 1986.

3. Goldman, Stuart. "The Legacy of Phobos 2," Sky and Telescope, 79: 15[illegible] (November 1990).

4. Jansson, Capt Scott W. Stable Orbits About the Martian Moons. MS Thesis, AFIT/GA/AA/89D-3. School of Engineering, Air Force Institute of Technology (AU), Wright Patterson AFB OH, December 1989.

5. Jordan, D.W. and P. Smith. Nonlinear Ordinary Differential Equations (Second Edition). New York: Oxford University Press, 1987.

6. Kubicek, M. and M. Marek. Computational Methods in Bifurcation Theory and Dissipative Structures. New York: Springer-Verlag New York Inc., 1983.

7. Meirovitch, Leonard. Methods of Analytical Dynamics. New York: Mcgraw-Hill Book Company, 1970.

8. Seydel, R. From Equilibrium to Chaos: Practical Bifurcation and Stability Analysis. New York: Elsevier Science Publishing Co., 1988.

9. Wiesel, William E. Advanced Astrodynamics. Lecture Notes for MC6.36, School of Engineering, Air Force Institute of Technology (AU), Wright Patterson AFB OH, December 1989.

Vita

Captain Frank Luria was born on February 22, 1963 in San Francisco, California. He graduated in 1981 from Lawrence Central High School, Indianapolis Indiana. He received the degree of Bachelor of Science in Astronautical Engineering from the U.S. Air Force Academy in 1985. His first assignment was to the Ballistic Missile Office, Norton AFB California. He worked in the Flight Test Division of the Advanced Strategic Missile Systems Directorate. Captain Luria entered the Air Force Institute of Technology in June of 1989. He and his wife, Renee, reside in Huber Heights, Ohio. They have a daughter, Ariel.

Permanent Address: 7425 East 51st Street
Indianapolis IN 46226

1990 December MS Thesis

Analysis of Periodic Orbits About the Martian Moons by Continuation Techniques

Frank Luria, Capt, USAF

School of Engineering
Air Force Institute of Technology
Wright Patterson AFB, Ohio 45433-6583

AFIT/GA/ENY/90D-10

From a few known periodic orbits of Phobos and Deimos, continuation techniques were used to find entire families of stable orbits. These techniques involved varying a parameter, the Hamiltonian, of the system and analyzing how the orbital behavior changed with the parameter. Floquet multipliers, for stability analysis, were also computed. AUTO86, a continuation/bifurcation software package, was used in this study. Artificial energy dissipation had to be added to the conservative Hamiltonian system to enable use of AUTO.

Orbits Phobos Continuation
Mars Deimos Bifurcation

74

UNCLASSIFIED UNCLASSIFIED UNCLASSIFIED Same as Report